The Planar Shape of Rock Joints

The Planar Shape of Rock Discontinuities

Lianyang Zhang[1, *], Herbert H. Einstein[2]

[1] *Department of Civil Engineering and Engineering Mechanics, University of Arizona, Tucson, Arizona, USA*

[2] *Department of Civil and Environmental Engineering, Massachusetts Institute of Technology, Cambridge, Massachusetts, USA*

Abstract

Knowing the planar shape of discontinuities is important when characterizing discontinuities in a rock mass. However, the real discontinuity shape is rarely known since the rock mass is usually inaccessible in three dimensions. Information on discontinuity shape is limited and often open to more than one interpretation. In this paper, a brief literature review about the shape of discontinuities is presented, including some information on discontinuity-surface morphology, inferences from observed trace lengths on different sampling planes, information based on experimental and theoretical studies, and discontinuity shapes assumed by different researchers. This review shows that discontinuities not affected by adjacent geological structures such as bedding boundaries or pre-existing fractures tend to be elliptical (or approximately circular but rarely). Discontinuities affected by or intersecting such geological structures tend to be rectangles. Using the general stereological relationship between trace length distributions and discontinuity size distributions developed by Zhang et al. (2002) for elliptical discontinuities, the effect of sampling plane orientation on trace lengths is then investigated. This study explains why the average trace lengths of non-equidimensional (elliptical or similar polygonal) discontinuities on two sampling planes can be about equal and thus the conclusion that rock discontinuities are equidimensional (circular) drawn from the fact that the average trace lengths

on two sampling planes are approximately equal can be wrong. Finally, methods for characterizing the shape and size of discontinuities (elliptical or rectangular) from trace length data are recommended and the appropriateness of using elliptical discontinuities to represent polygonal, especially rectangular, discontinuities is discussed.

1. INTRODUCTION

Research results have shown that the planar shape of discontinuities (fractures or joints)[*] has a profound effect on the connectivity of discontinuities and on the strength, deformability and permeability of rock masses (e.g., Petit et al. 1994; Dershowitz 1998; Zhang 1999, 2005). Consequently, it is important to know the planar shape of discontinuities when characterizing them in a rock mass. However, the real discontinuity shape at a site is rarely known since a rock mass is usually inaccessible in three dimensions. Information on discontinuity shape is limited and often open to more than one interpretation (Warburton 1980a; Wathugala 1991). Dershowitz and Einstein (1988) stated: "Shape of joint boundaries can be polygonal, circular, elliptical or irregular. Joints can be planar or non-planar in space and shape should consider this fact also. Since joints are often planar, it is simpler to associate 'shape' with the two-dimensional appearance and treat non-planarity separately." This paper mainly discusses the shape of planar discontinuities but makes some comments on discontinuity surface morphology.

Discontinuities can be classified into two categories: unrestricted and restricted. Unrestricted discontinuities are effectively isolated and their growth has not been limited by adjacent

[*] Discontinuity, fracture and joint will be used interchangeably as is the case in the literature.

geological structures such as other discontinuities and bedding boundaries [see Fig. 1(a)]. In general, the edge of unrestricted discontinuities is or can be approximated by a closed convex curve. In many cases, the growth of discontinuities is limited by adjacent preexisting discontinuities or bedding planes and free surfaces. Fig. 1(b) shows such a restricted discontinuity, in principle, while Fig. 1(c) shows an actual example of so called layer perpendicular joints, a type of restricted discontinuity. Such discontinuities are called restricted discontinuities (fractures). One way to represent restricted discontinuities is to use polygons, where some of the polygon sides are formed by intersections with the adjacent preexisting discontinuities and/or bedding boundaries.

In this paper, first a brief literature review about the planar shape of discontinuities is presented, including some information on fracture-surface morphology, inferences from observed trace length data on different sampling planes, information based on experimental and theoretical studies, and discontinuity shapes assumed by different researchers. This is followed by the analysis of the available data, the investigation of the effect of sampling plane orientation on trace lengths, and the discussion of the appropriateness of using elliptical discontinuities to represent polygonal, especially rectangular, discontinuities or vice versa. Finally, methods for characterizing the shape and size of discontinuities (elliptical or rectangular) from trace length data are presented.

2. FIELD OBSERVATIONS ON DISCONTINUITY SHAPE

Joint shape has been of interest to geologists and has thus been studied for quite some time. One of the earliest and often cited literature references regarding joint geometry is Woodworth's (1896) study of joints in Cambridge Argillite (a slightly metamorphosed shale) which he calls pelite, to indicate that its structure is that of the original stratification. He did this study to show that joints are not infinite planar surfaces but that they have a distinct surface morphology and a finite shape. In the former, he distinguishes the central part with feather structures/texture called "joint plane" surrounded by the "joint fringe". The joints in the fringe differ distinctly in orientation from the joint plane, they consist of an echelon joints, so called b- (boundary) joints often cut at a right angle by c (cross) joints. All this is shown in Fig. 2. In addition, there may be a boundary of conchoidal fractures surrounding the fringe. With regard to shape, Woodworth mentioned (and showed, see also Fig. 2) that the joints he studied, which had sizes in the order of 200 mm, were elliptically shaped. In addition, he observed smaller (1/2 to 2 inches diameter) so called discoid joints of circular/elliptical shape. Woodworth (1896), by the way, mentions that feather surface morphology can also be observed in a variety of igneous rocks. It may be worthwhile mentioning that Hodgson (1961) refined Woodworth's information by distinguishing systematic and non-systematic joints on the basis of surface morphology. Hodgson does mention briefly that "most systematic joints are elliptical in shape, ranging from very elongated to moderately elongated in the direction of the plane axis". He then goes on to say that surface structure is rarely radial (plumose structures emanating from a point and producing a circular joint). Hodgson (1961) finally comments on cross-joints, one of the non-systematic joints, and states that they extend between systematic joint and often

terminate against other non-systematic or systematic joints. One can infer from this, but Hodgson does not say so, that such cross joints will have a rectangular shape.

Another early set of detailed observations on fracture surfaces and shapes are those by Bankwitz (1965). Fig. 3 shows the fracture morphology consisting of plumose features in the center part (Hauptkluft after Bankwitz), radial features (Radialklüfte after Bankwitz) and stepped boundary features (Randklüfte after Bankwitz). (This subdivision is to some extent similar to that by Woodworth – the Hauptkluft corresponds to Woodworth's joint plane, while the "Radial" - and "Randklüfte" together correspond to Woodworth's fringe.) The morphology is mentioned here since similar to Woodworth, one of the main interests of Bankwitz in this and the following papers (Bankwitz 1966, 1978; Bankwitz and Bankwitz 1984) is the fact that fractures are not planar but three-dimensional features. He shows a systematic sketch of fracture development in his next paper (Bankwitz 1966) which is reproduced in Fig. 4. The fact that fractures are or can be three-dimensional has to be kept in mind; in other words, the assumption of planarity is a simplification, although an acceptable one in the context of this paper. Another reason why this is mentioned is that the features shown in Fig. 3 are characteristic of tensile fractures. This and the difference to shear related fractures has been discussed e.g. by Einstein and Dershowitz (1988) but also by many others (e.g., Cloos 1955; Einstein and Dershowitz 1990; Einstein and Bobet 2004; Gross et al. 1997; Hoek 1968; Horii and Nemat-Nasser 1986; Lajtai 1969; Pollard and Aydin 1988; Price 1966; Riedel 1929; Saltzman 2001; Sheldon 1912).

After these initial comments about surface morphology, we will now concentrate on Bankwitz's (1965, 1966) comments on shape. Bankwitz (1965) did these studies in the "Thüringer Schiefergebirge" with a variety of metamorphic lithologies (different schists, quartzite) but also considering igneous intrusions (diabase, granite). His statement about fracture shape is quoted here (translated from German):

"The fractures in an outcrop are normally a series of either elliptical (ideally circular) [fractures] and have a natural termination in the rock, or – and this holds for the greater number – they end at other fractures, bedding or schistocity surfaces, etc. The latter have, therefore, linear boundaries. To the problem of fracture genesis, the first group is very important."

These "classic" early studies on discontinuity shape (Woodworth 1896; Bankwitz 1965 and later) therefore, indicate that one rarely sees circular shapes and often sees elliptical shapes, where elongated ellipses may be caused by boundary layers. In addition, rectangular shapes can also be observed, particularly if bounded by existing joints.

More recent studies, in which elliptical joint shapes were reported, are those by Kulander et al. (1979), Bahat (1988), Petit (1994), Weinberger (2001), Bahat et al. (2003) and Savalli and Engelder (2005).

Weinberger (2001) analyzed the surface morphology of joints in the dolomite layers of the Judea Group, Israel in order to study the role played by spherical cavity-shaped flaws during nucleation and growth of joints. He found that joints typically show two forms of growth,

depending on the abundance and spatial distribution of cavities within the layers. In layers with many cavities, joints preferably initiate at critical cavities, propagate vertically toward bedding interfaces and horizontally toward adjacent joints, and form elliptical fractures. In layers free of cavities, joints initiate at bedding interfaces, commonly propagate downward toward the layer base and adjacent joints, and form semi-elliptical fractures. In both cases, the joint propagation is impeded by the bedding interfaces between the dolomite layers.

Bahat et al. (2003) studied the joints in the Borsov granite based on analyses of joint-surface morphology of 10 exposed joints in a quarry. The study area is located in the South Bohemian Pluton. The results show that the joints in the Borsov granite have a mirror plane (a smooth crack surface that contains the initial and critical flaws, the striae, and the undulations), which is either (approximately) circular or elliptical. For joints with exposed boundaries, the mirror planes deviate from circularity into various ellipses (see Fig. 5).

Savalli and Engelder (2005) studied the mechanisms controlling rupture shape during the growth of joints in layered clastic rocks based on field observations of exposed joints. In layered rocks, a rupture can initiate either from the interior of a bed or from the bed boundary, which is similar to the conclusion drawn by Weinberger (2001) discussed above. Maps of tip line profiles during early joint growth (before intersecting the bed boundary) delineate (approximately) circular and elliptical rupture shapes. For homogeneous and isotropic rock, the velocity of the crack tip line is equal in all directions at the onset of rupture and the rupture shape during early joint growth will be simply circular. Since natural rock is usually inhomogeneous and anisotropic, the rupture shape during early joint growth will not be

(perfectly) circular. After the joint intersects the bed boundary(ies), the crack tip line will split into two discontinuous moving segments and the two separate tip lines will move synchronously away from each other, forming (approximately) elliptical or rectangular rupture shape (see Fig. 6).

A study of particular interest regarding the differentiation between elliptical (possibly circular) and rectangular joints is that by Petit et al. (1994). They studied joints in the Permian sandstones of the Lodève basin in France, which consist of relatively massive pelites and isolated sandstone layers within the pelite. As will be seen later, the joint characteristics in pelite and sandstone are quite different. Before summarizing what Petit et al. observed, it is interesting to note that they initiated this field study because they were dissatisfied with mostly mathematically oriented preceding studies leading to randomly distributed (circular?) disks. Petit et al. concentrated on Mode I fractures. In the pelites, a steeply dipping set of joints was observed, specifically the vertical extent H and the horizontal extent L, which they backfigured from joint traces visible on 10 to 15° inclined outcrops. Statistics based on 55 measurements gave L_{mean} = 5.1 m, H_{mean} = 2.7 m both showing lognormal distribution. This results in an aspect ratio of L/H = 1.9. Petit et al. also explicitly observed several isolated ellipses (with plumose surface features, etc.) of similar aspect ratio (2.0). They conclude that excluding some circular and some elongated features, one can assume a general elliptical form for fractures in the pelites. In addition, they observed abutting fractures (geometry limited by existing fractures), which are apparently rectangular with higher L/H. In the isolated sandstone layers, however, the result was quite different. These measurements were made in two beds where the

bed thickness corresponds to joint height H, while joint trace length L was measured as such. The results were as follows: $L/H > 5.0$ and $L/H > 4.0$ and definitely of rectangular form.

Locsin (2005) in the context of developing models for "layer perpendicular" joints studied a number of cases, mostly in sedimentary rocks. Layer perpendicular joints occur in rocks where the layers differ in stiffness and where, as a consequence, jointing occurs mostly in the stiffer layer. The cases studied were those reported by Becker and Gross (1996) and by Saltzman (2001) on the limestone/dolostone Gerofit formation in Israel, by Gross et al. (1997) on six interbedded chalk/chert layer near Beersheva (Israel) and by Baudo (2001) on sandstones and shales of the Upper Canadaway formation exposed along Cattavaugus Creek in Southwestern New York State. The vertical height of the joint traces in all these cases are equal to the thicknesses of the jointing layers, i.e. for the limestone/dolostone Gerofit formation in Becker and Gross (1996) and Saltzman (2001) between 0.12 and 0.52 m, for the chalk in Gross et al. (1997) between 0.17 and 0.63 m, and for the sandstone/schistose layer in Baudo (2001) 0.09 m while for the three other sandstone layers in Baudo (2001) this is 0.1 m. In all cases, the beds/layers are flatly dipping or horizontal. While no or only very limited measurements of horizontal trace lengths have been reported, one can infer from the information on bed thickness, (equal to joint height), and bed orientation and geologic setting that the joints are essentially rectangular with large aspect ratios. These are again all cases where there is a strong boundary effect in that the jointing layer is usually stiffer than the bounding non-jointing layer.

Many other articles and reports have appeared in the last three decades discussing possible shapes of discontinuities based on in-situ trace length data:

1. Robertson (1970), after analyzing nearly 9,000 traces from the De Beer mine, South Africa, concluded that the strike trace length and the dip trace length of discontinuities have about the same distribution, possibly implying discontinuities to be equidimensional (circular). Fig. 7 shows the strike and dip traces of a discontinuity.
2. Bridges (1975) stated that "there is good evidence for" individual discontinuities to be taken to have a rectangular (elongated) shape, especially for discontinuities in anisotropic rock. However, no specific data can be found in the original paper to support this statement.
3. Barton (1977) presented a geotechnical analysis of rock structure and fabric at the C.S.A. Mine, Cobar, New South Wales. The country rock within the mine area is overwhelmingly composed of chloritic and quartzitic siltstone to slaty claystone. Based on observations of trace lengths of discontinuities visible on wall photographs of cross cuts, Barton (1977) concluded that discontinuities are approximately equidimensional.
4. Einstein et al. (1979) investigated discontinuities at a site in southern Connecticut. The country rock at this site is the Monson Gneiss, a thinly banded rock with feldspathic and biotitic layers. There are two major discontinuity sets at this site. Set 1 dips steeply to the southeast and Set 2 is nearly horizontal. Trace lengths of discontinuities were measured on both the horizontal and vertical surfaces of excavations. The results indicate that discontinuities are non-equidimensional (see Table 1).
5. According to Mostyn and Li (1993), McMahon (1982) used a dip length equal to 60% of the strike length for discontinuities in slope design. Since the original paper of McMahon (1982) is not accessible, it is not clear if**,** but can be assumed that McMahon based this ratio on in-situ data.

Rippon (1985a, b), Barnett et al. (1987), Walsh and Watterson (1987) and Nicol et al. (1996) have shown that simple normal faults have an approximately elliptical shape with the major axis sub-horizontal. The ellipticity of simple normal faults can "be due either to the mechanical heterogeneity of the rock sequence, or to the energy differences between screw and edge dislocations which would result in elliptical fault surfaces even in mechanically isotropic rock" (Nicol et al. 1996). Nicol et al. (1996) examined the throw contour diagrams of 35 normal faults and presented their principal dimensions as shown in Fig. 8 and Table 2. The aspect (major to minor axis) ratios of these fault surfaces range from 1.0 to 3.4 with a mean of 2.15. Please note that the average aspect ratios listed in Table 2 are for faults at each site.

From all the above, one can infer that discontinuities formed in extension (mode I fractures/joints or normal faults) have elongated shapes where these shapes can be either elliptical or rectangular (occasionally other polygonal shapes). Circular disks can occur but do so rarely, and they can be considered special cases of ellipses.

3. DISCONTINUITY SHAPE BASED ON EXPERIMENTAL AND THEORETICAL STUDIES

Researchers have also studied the shape of discontinuities experimentally and theoretically. Daneshy (1973) experimentally investigated the shape of hydraulically induced fractures in hydrostone and limestone by studying fracture characteristics: facial features, hackle marks, and rib marks. The experiments were conducted on rectangular blocks of 152 mm by 152 mm by 254 mm. A borehole of 254 mm long and 7.95 mm in diameter was drilled from the center of

the top square to the center of the bottom square. Two steel tubings of equal length were then cemented at the top and the bottom of the borehole. Different heights of the open-hole part were obtained by changing the lengths of the casings. Fractures were then induced by injecting fluid into the borehole. The results indicate that hydraulic fractures extending from a point source (very short open-hole part) propagate radially, with their edge having a circular shape. The fractures extending from a line source (long open-hole part), however, propagate on a hyperbolic path, with their edge having an elliptical shape. As the elliptical fracture propagates further, the shape of the fracture tends more and more towards being circular.

Moriya et al. (2006) examined the propagation of fractures at the Bernburg salt mine by analyzing hydraulically induced acoustic emissions (AE). The results show that the AE source locations are distributed as an ellipse and the principal direction of the source distribution changes according to the change of the principal stress direction, indicating that the shape of the fracture is elliptical (see Fig. 9).

Moriya et al. (2006) also examined the propagation of fractures based on fracture mechanics analysis. Considering a two-dimensional elliptical fracture in a homogeneous and isotropic elastic medium (see Fig. 10) and assuming uniform normal stress and shear stress acting on the fracture, Moriya et al. (2006) derived the energy release rate G as follows

$$G(\phi,k)=\frac{1-\nu^2}{2E}\pi b\{\frac{\sigma^2}{[E(k')]^2}(1-k'^2\cos^2\phi)^{1/2} + \frac{\tau^2}{B^2}[\frac{\cos^2\phi}{k^2}+(1-\nu)\sin^2\phi]\frac{k'^2}{(1-k'^2\cos^2\phi)^{1/2}}\} \quad (1)$$

in which E and ν are respectively the elastic modulus and Poisson's ratio of the rock; k (= a/b) is the aspect ratio, where a and b are respectively the major and minor axis length of the elliptical fracture; σ and τ are respectively the normal and shear stress acting on the fracture; ϕ is the eccentric angle (see Fig. 10); and

$$k' = 1 - (1/k)^2 \tag{2}$$

$$B = (k'^2 - \nu)E(k') + \nu K(k')/k^2 \tag{3}$$

$$E(k') = \int_0^{\pi/2} \sqrt{1 - k'^2 \sin^2 \phi}\, d\phi \tag{4}$$

$$K(k') = \int_0^{\pi/2} \frac{d\phi}{\sqrt{1 - k'^2 \sin^2 \phi}} \tag{5}$$

So the energy release rate is simply a function of the eccentric angle ϕ and aspect ratio k for given normal stress σ and shear stress τ. Fig. 11 shows the energy release rate for the case of σ/τ = 1/3. In this case, when the aspect ratio is greater than 1.30, say 10, the highest energy release rate occurs at ϕ = 90°, meaning that the fracture mostly tends to grow in the direction of the minor axis of the fracture and the aspect ratio will be decreased. If the aspect ratio (a/b) is smaller than 1.30, say 1.11, on the other hand, the highest energy release rate occurs at ϕ = 0°, meaning that the fracture mostly tends to grow in the direction of the major axis of the fracture and the aspect ratio will be increased. For an aspect ratio of 1.30, the energy release rate is constant for all directions, which suggests that the fracture expands in all directions, preserving the aspect ratio of 1.30. So for the case of σ/τ = 1/3, the converging aspect ratio of the elliptical fracture is 1.30. For other values of stress ratio σ/τ, the corresponding converging aspect ratios of the elliptical fracture were also determined by Moriya et al. (2006) (see Fig. 12). It can be seen that a fracture mainly subjected to shear stress (very small σ/τ) is likely to propagate to a

fracture with an aspect ratio of 1.33. On the other hand, the extension of a fracture subjected only to normal stress (very large σ/τ) is likely to be circular.

Although the simple assumptions made by Moriya et al. (2006) may not be representative of real conditions, **his** results **indicate** that (unbounded) fractures tend to be elliptical when shear stress is available.

5. ASSUMPTIONS ABOUT THE DISCONTINUITY SHAPE BY DIFFERENT RESEARCHERS

Researchers have assumed different discontinuity shapes for different research and application puposes. Due to the mathematical convenience, many investigators assume that discontinuities are thin circular discs randomly located in space (Baecher et al. 1977; Warburton 1980a; Chan 1986; Villaescusa and Brown 1990; Kulatilake et al. 1993; Song and Lee 2001; Song 2006). Baecher later extended his model to also include elliptical discontinuities (Einstein et al. 1979).

With circular discontinuities, the trace patterns in differently oriented sampling planes will be the same. In practice, however, the trace patterns may vary with the orientation of sampling planes (Warburton 1980b). Therefore, Warburton (1980b) assumed that discontinuities in a set are parallelograms of various sizes. Kulatilake et al. (1990) not only considered discontinuities as circular disks but as rectangles, squares, right triangles, parallelograms, rhombuses and oblique triangles in their study of the effect of joint orientation, joint size and joint shape on the statistical distribution of the orientation.

Dershowitz et al. (1993) used polygons to represent discontinuities in his discrete fracture code. The polygons are formed by inscribing a polygon in an ellipse (see Fig. 13). Ivanova (1995, 1998) and Meyer (1999) also used polygons to represent discontinuities in their discrete fracture code. It is noted that polygons can be used to effectively represent elliptical discontinuities when the number of polygon sides is large (Dershowitz et al. 1993) or vice versa.

Zhang et al. (2002) considered discontinuities to be ellipses and derived the general stereological relationship between trace length distribution and discontinuity size (represented by the major axis length of the ellipse) distribution. Based on the general stereological relationship, they investigated the effect of sampling plane orientation on trace lengths and proposed a method for inferring the size distribution of elliptical discontinuities from trace length sampling on different sampling planes.

6. ANALYSIS OF EXISTING INFORMATION ON DISCONTINUITY SHAPE

As discussed above, discontinuities not affected by adjacent geological structures such as bedding boundaries tend to be elliptical (or approximately circular but rarely). Discontinuities affected by or intersecting geological structures such as bed boundaries and other fractures tend to be rectangles.

Some researchers infer the discontinuity shape from the study of trace lengths on two (usually perpendicular) sampling planes. However, inferring discontinuity shape based only on trace lengths on two sampling planes may lead to wrong conclusions. For example, the fact that the average trace lengths of a discontinuity set on two perpendicular sampling planes are equal does

not necessarily mean that the discontinuities of such a set are equidimensional; instead, there exist the following three possibilities (Zhang et al. 2002):

a) The discontinuities are indeed equidimensional [see Fig. 14(a)].
b) The discontinuities are non-equidimensional such as elliptical or rectangular with long axes in a single (or deterministic) orientation. However, the two perpendicular sampling planes are oriented such that the trace lengths on them are approximately equal [see Fig. 14(b)].
c) The discontinuities are non-equidimensional such as elliptical or rectangular with long axes randomly oriented. The two perpendicular sampling planes are oriented such that the average trace lengths on them are approximately equal [see Fig. 14(c)].

Therefore, the conclusion that discontinuities are equidimensional (circular) drawn from the fact that the average trace lengths of a discontinuity set on two sampling planes are about equal is questionable. On the other hand, if the average trace lengths of a discontinuity set on two sampling planes differ greatly, it can be concluded that the discontinuities are non-equidimensional. The following is a more detailed discussion on the effect of sampling plane orientation on the trace lengths.

Assuming elliptical discontinuity shapes, Zhang et al. (2002) derived the general stereological relationship between trace length distribution $f(l)$ and discontinuity size (expressed by the major axis length a of the ellipse) distribution $g(a)$ for area (or window) sampling:

$$f(l) = \frac{l}{M\mu_a} \int_{l/M}^{\infty} \frac{g(a)}{\sqrt{(Ma)^2 - l^2}} da \qquad (l \le aM) \tag{6}$$

where l is the length of a trace; μ_a is the mean of major axis length a; and M is a factor which can be determined by

$$M = \frac{\sqrt{\tan^2 \beta + 1}}{\sqrt{k^2 \tan^2 \beta + 1}} \tag{7}$$

in which $k = a/b$ is the aspect ratio of the discontinuity; and β is the angle between the discontinuity major axis and the trace line (note that β is measured in the discontinuity plane) (see Fig. 15). Obviously, β will change for different sampling planes. For a specific sampling plane, however, there will be only one β value for a discontinuity set with a deterministic orientation.

Based on equation (6), Zhang et al. (2002) derived expressions for determining the mean μ_l and standard deviation σ_l of trace lengths from the mean μ_a and standard deviation σ_a of discontinuity size a, respectively for the lognormal, negative exponential and Gamma distribution of discontinuity size a (see Table 3) (a is the major axis length of an elliptical discontinuity).

Using the expressions in Table 3, one can investigate the effect of sampling plane orientation on trace lengths. Fig. 16 shows the variation of the mean and standard deviation of trace lengths with β, respectively for the lognormal, negative exponential and Gamma distribution of discontinuity size a. For other distribution forms of discontinuity size a, similar figures can be

obtained. Since β is the angle between the trace line and the discontinuity major axis, it is related to the sampling plane orientation relative to the discontinuity. It can be seen that, for all the three distribution forms of discontinuity size *a*, there are extensive ranges of sampling plane orientations, reflected by β, over which both the mean and standard deviation of trace lengths show little variation, especially for large *k* values; this is so despite the considerable difference between the maximum and the minimum, respectively, of the mean and standard deviation of trace lengths.

The results in Fig. 16 could well explain why Bridges (1976), Einstein et al. (1979) and McMahon (Mostyn & Li, 1993) found different mean trace lengths on differently oriented sampling planes, whereas Robertson (1970) and Barton (1977) observed them to be approximately equal. In each of these reports, the number of differently oriented sampling planes was very limited and, depending on the relative orientations of the sampling planes, the authors could observe either approximately equal mean trace lengths or significantly different mean trace lengths. For example, in Bridges (1976), Einstein et al. (1979) and McMahon (Mostyn & Li, 1993), the two sampling planes might be respectively in the $\beta = 0° - 20°$ (or $160° - 180°$) range and the $\beta = 40° - 140°$ range, or vice versa. From Fig. 16, this would result in very different mean trace lengths. On the other hand, in Robertson (1970) and Barton (1977), the two sampling planes might be both in the $\beta = 40° - 140°$ range (i.e., in the "flat" trace length part of Fig. 16) or respectively in some β ranges approximately symmetrical about $\beta = 90°$. It should be noted that the comments above are simply assumptions because no information about the β values can be found in the original papers or reports.

7. DETERMINATION OF DISCONTINUITY SHAPE FROM TRACE DATA

The discussion of observed discontinuity shapes has shown that some discontinuities are elliptical (possibly circular but rarely). Such discontinuities occur in unbounded or weakly bounded rock. On the other hand, bounded discontinuities are usually rectangular. To determine discontinuity shape from discontinuity traces, the following general two-step process can be followed:

Step 1. Evaluation of geologic information

Based on geologic information, decide if the fracture can be approximated by an ellipse or a rectangle. Discontinuities not affected by adjacent geological structures such as bedding boundaries or pre-existing fractures tend to be elliptical but discontinuities affected by or intersecting such geological structures tend to be rectangles.

Step 2. Characterize discontinuities from discontinuity traces

Based on measured trace lengths on different sampling planes, discontinuities can be characterized following the procedures in Sections 7.1 and 7.2 respectively for elliptical and rectangular discontinuities.

7.1. Characterization of elliptical discontinuities

For elliptical discontinuities, the procedure of Zhang et al. (2002) as outlined below can be followed to estimate discontinuity shape and size:

(a) Obtain the trace length data on different sampling window (outcrops).

(b) Assume a major axis orientation and compute the β (the angle between discontinuity major axis and trace line) value for each sampling window (see Fig. 15).

(c) For the assumed major axis orientation, compute μ_a and σ_a of the discontinuity size, using expressions derived from the general stereological relationship (Eq. 6), from the trace length data of each sampling window, by assuming different aspect ratios k and different distribution forms of $g(a)$. The results are then used to draw the curves relating μ_a (and σ_a) to k, respectively, for the assumed distribution forms of $g(a)$ (see, e.g., Fig. 17 for assumed lognormal distribution of $g(a)$).

(d) Repeat steps (b) and (c) until the curves relating μ_a (and σ_a) to k for different sampling windows intersect in one point (see, e.g., Fig. 17). The major axis orientation for this case is the inferred actual major axis orientation. The k, μ_a and σ_a values at the intersection points are the corresponding possible characteristics of the discontinuities.

7.2. Characterization of rectangular discontinuities

For rectangular discontinuities, one of the following three methods can be used to characterize discontinuity shape and size. It is also possible to combine two or all of the three methods for the characterization.

Method 1: Simply measure the discontinuity traces on bedding faces and bedding tops and geometrically infer rectangles based on simple geometry. The characterization of joints in isolated sandstone layers by Petit et al. (1994) can be considered an example of this method.

Method 2: Follow the procedure of Zhang et al. (2002) as described in Section 7.1 to estimate discontinuity shape and size; but the stereological relationship specifically for rectangular discontinuities will be used. For example, the general stereological relationship between trace length distribution and discontinuity size distribution derived by Warburton (1980b) for parallelograms can be used, a rectangle being a parallelogram with right angles. Using Warburton's stereological relationship, the expressions for determining the mean and standard deviation of discontinuity size from the mean and standard deviation of trace lengths can be derived for different distributions of discontinuity size. In these expressions, the orientation of a sampling window is defined by the angle between a side of the rectangle and the trace line. With these derived expressions, the procedure of Zhang et al. (2002) can then be used estimate the discontinuity shape and size.

Method 3: Treat rectangular discontinuities as ellipses at the same aspect ratio and follow the procedure of Zhang et al. (2002) as described in Section 7.1 to estimate discontinuity shape and size. The appropriateness of using ellipses to represent rectangular discontinuities is discussed in Section 7.3.

7.3. Using ellipses to represent rectangular discontinuities

Consider an ellipse and a rectangle which have the same area and the same aspect ratio (see Fig. 18), i.e.

$$\pi ab/4 = LW \tag{8}$$

$$a/b = L/W = k \tag{9}$$

where a and b are respectively the major and minor axis length of the ellipse; and L and W are respectively the length and width of the rectangle. From Eqs. (8) and (9), L and W can be related respectively to a and b as follows

$$L = \frac{\sqrt{\pi}}{2} a = 0.87a \tag{10}$$

$$W = \frac{\sqrt{\pi}}{2} b = 0.87b \tag{11}$$

If the centers of the ellipse and rectangle are at the same location and their major axes are in the same direction, the area of the rectangle covered by the ellipse (the shaded area in Fig. 15) can be obtained as

$$A_c = \frac{ab}{2}\left[\sqrt{\pi}\frac{\sqrt{4-\pi}}{2} + \sin^{-1}\left(\frac{\sqrt{\pi}}{2}\right) - \sin^{-1}\left(\frac{\sqrt{4-\pi}}{2}\right)\right] \tag{12}$$

So the ratio of the covered area to the total area of the rectangle is

$$\frac{A_c}{A_t} = \frac{2}{\pi}\left[\sqrt{\pi}\frac{\sqrt{4-\pi}}{2} + \sin^{-1}\left(\frac{\sqrt{\pi}}{2}\right) - \sin^{-1}\left(\frac{\sqrt{4-\pi}}{2}\right)\right] = 0.91 \tag{13}$$

A ratio greater than 0.91 will result for discontinuities bounded by straight bedding boundaries but having curved ends such as those shown in Figs. 5 and 6.

One can thus state that since the ellipse covers over 90% of the rectangle, it is usually appropriate to use elliptical discontinuities to represent rectangular discontinuities. Using an elliptical approximation has the advantage that its size and shape can be obtained from trace length data (as proposed by Zhang et al., 2002). This holds even more for polygonal discontinuities with a larger number of sides, say > 5. Clearly, the reverse, i.e. multisided

polygons can be used to represent ellipses is also applicable (see Fig. 13). This may be one of the reasons why polygons are used to represent discontinuities in discrete fracture codes.

8. SUMMARY AND CONCLUSIONS

A brief literature review about the shape of rock discontinuities has been conducted. In the literature, some actual observations of discontinuity shape have been made based on information on discontinuity surface-morphology while many researchers have used trace length observations to approximately infer discontinuity shapes. Researchers have also conducted experimental and theoretical studies on the shape of discontinuities. The literature review is followed by the analysis of the available data, the investigation of the effect of sampling plane orientation on trace lengths, the discussion of the appropriateness of using elliptical discontinuities to represent polygonal discontinuities, and the presentation of methods for characterizing discontinuity shape and size from trace length data. Based on the analysis and investigation results, the following conclusions can be drawn:

1) Discontinuities not affected by adjacent geological structures such as bedding boundaries tend to be elliptical (or approximately circular but rarely), while discontinuities affected by or intersecting geological structures such as bed boundaries tend to be most likely rectangles or similarly shaped polygons.
2) Even for non-equidimensional (elliptical or rectangular) discontinuities, the average trace lengths on two sampling planes can be about equal. So the conclusion that rock discontinuities are equidimensional (circular) drawn from the fact that the average trace lengths on two sampling planes are approximately equal can be wrong.

3) To estimate the shape and size of elliptical discontinuities from trace length data, the procedure of Zhang et al. (2002) can be followed.
4) Rectangular discontinuities can be characterized by simple measurements of discontinuity traces on bedding faces and bedding tops and geometrical inferences based on simple geometry. The general stereological relationship between trace length distribution and discontinuity size distribution for rectangular discontinuities can also be used to characterize rectangular discontinuities by following the procedure of Zhang et al. (2002). Since elliptical discontinuities can be used to reasonably represent polygonal including rectangular discontinuities or vice versa, the shape and size of rectangular discontinuities can be estimated from trace length data by treating them as elliptical discontinuities and again following the procedure of Zhang et al. (2002).

REFERENCES

Baecher, G. N., Lanney, N. A., and Einstein, H. H. (1977). "Statistical description of rock properties and sampling." *18th U.S. Symp. on Rock Mechanics*, 5C1-8.

Bahat, D. (1988). "Fractographics determination of joint length distribution in chalk." *Rock Mechanics and Rock Engineering*. 21(1), 79-94.

Bahat, D., Bankwitz, P., and Bankwitz, E. (2003). "Preuplift joints in granites: Evidence for subcritical and postcritical fracture growth." *GSA Bulletin*, 115(2), 148-146.

Bankwitz, P. (1965). “Ueber Kluefte: I. Beobachtungen im Thuringischen Schiefergebirge.” *Geologie*, 14, 241–253.

Bankwitz, P. (1966). “Ueber Kluefte: II. Die Bildung der Kluftoberflaeche und eine Systematik ihrer Strukturen.” *Geologie*, 15, 896–941.

Bankwitz, P. (1978). “Ueber Kluefte: III. Die Entstehung von Saulenkluften.” *Zeitschrift Geol. Wissenschaften*, 6, 285-299.

Bankwitz, P., and Bankwitz, E. (1984). “Beitrag zur Interpretation von Rupturen.” *Zeitschrift fur Angewandte Geologie*, 30, 265-271.

Barnett, J. A. M., Mortimer, J., Rippon, J., H., Walsh, J. J., and Watterson J. (1987). “Displacement geometry in the volume containing a single normal fault.” *Bull. Am. Ass. Petrol. Geol*., 71, 925-937.

Barton, C. M. (1977). “Geotechnical analysis of rock structure and fabric in CSA Mine NSW.” *Applied Geomechanics Technical Paper 24*, Commonwealth Scientific and Industrial Research Organization, Australia.

Baudo, A. (2001). 1-*D Fractal, Geostatistical and abusing analyses of fractures along a 4 km scanline*. M.S. Thesis, The State University of New York at Buffalo.

Becker, A., and Gross, M. R. (1996). "Mechanism for joint saturation in mechanically layered rocks: an example from Southern Israel." *Tectonophysics*, 257, 223-237.

Bridges, M. C. (1976). "Presentation of fracture data for rock mechanics." *2nd Australia-New Zealand Conf. on Geomechanics*, Brisbane, 144-148.

Chan, L. P. (1986). "Application of Block Theory and Simulation Techniques to Optimum Design of Rock Excavations." Ph.D. thesis, University of California, Berkeley.

Cloos, E. (1955). "Experimental Analysis of Fracture Patterns." *Geol. Soc. Am. Bull*., 66 (3), 241-256.

Daneshy, A. A. (1973). "Three-dimensional propagation of hydraulic fractures extending from open holes." *Application of Rock Mechanics - 15th Symposium on Rock Mechanics*, Custer State Park, SD, 157-179.

Dershowitz, W. S. (1998). *Discrete feature approach for heterogeneous reservoir production enhancement.* Progress Report: October 1, 1998 – December 31, 1998, Golder Associates Inc.

Dershowitz, W. S., and Einstein, H. H. (1988). "Characterizing rock joint geometry with joint system models." *Rock Mechanics and Rock Engineering*, 21, 21-51.

Dershowitz, W. S, Lee, G., Geier, J., Foxford, T., LaPointe, P., and Thomas, A. (1993). FracMan, Interactive discrete feature data analysis, geometric modeling, and exploration simulation. User Documentation, Version 2.3, Golder Associates Inc., Seattle, Washington.

Einstein, H. H., Baecher, G. B., and Veneziano, D. (1979). *Risk Analysis for Rock Slopes in Open Pit Mines – Final Technical Report,* Parts I-V, USBM J 027 5015, Department of Civil Engineering, MIT, Cambridge, Massachusetts.

Einstein, H. H., and Bobet, A. (2004). "Crack Coalescence in Brittle Materials: An Overview." *EUROCK 2004 &53rd Geomechanics Colloquium*, Schubert (ed.).

Einstein, H. H., and Dershowitz, W. S. (1990). "Tensile and Shear Fracturing in Predominantly Compressive Stress Fields – a Review." *Eng. Geology*, 29, 149-172.

Gross, M.R., Bahat, D., and Becker, A. (1997). "Relations between jointing and faulting based on fracture-spacing ratios and fault-slip profiles: a new method to estimate strain in layered rocks." *Geology*, 25(10), 887-890.

Hodgson, R. A. (1961). "Classification of Structures on Joint Surfaces." *Am. J. of Science*, 259, 493-502.

Hoek, E. (1968). "Brittle Fracture of Rock." *Rock Mechanics in Engineering Practice*, K.G. Stagg and O.C. Zienkiewicz (Editors), Wiley. 99-124.

Horii, H., and Nemat-Nasser, S. (1986). "Brittle Failure in Compression: Splitting, Faulting and Brittle Ductile Transition." *Phil. Trans. R. Soc. London, Math. Phys. Sci.*, 319 (1549).

Ivanova, V. (1995). *Three-dimensional stochastic modeling of rock fracture systems*. MS thesis, Massachusetts Institute of Technology, Cambridge, MA.

Ivanova, V. (1998). *Geologic and stochastic modeling of fracture systems in rocks*. PhD thesis, Massachusetts Institute of Technology, Cambridge, MA.

Kulander, B. R., Barton, C. C., and Dean, S. L. (1979). *The Application of Fractography to Core and Outcrop Fracture Investigations*, U.S. Dept. of Energy Report METC/SP-79/3, Morgantown Energy Research Center, pp. 175.

Kulatilake, P. H. S. W., Wathugala, D. N., and Stephansson, O. (1993). "Stochastic three dimensional joint size, intensity and system modeling and a validation to an area in Stripa Mine, Sweden." *Soils and Foundations*, 33(1), 55-70.

Kulatilake, P. H. S. W., Wu, T. H., and Wathugala, D. N. (1990). "Probabilistic modeling of joint orientation." *Int. J. Num. Anal. Method Geomech.*, 14, 325-250.

Lajtai, E. Z. (1969). "Strength of Discontinuous Rocks in Direct Shear." *Geotechnique*, 19 (2), 218-223.

Locsin, J. L. Z. (2005). *Modeling Joint Patterns Using Combinations of Mechanical and Probabilistic Concepts*. Ph.D. Thesis. Massachusetts Institute of Technology, Cambridge, MA.

Meyer, T. (1999). Geologic stochastic modeling of rock fracture systems related to crustal faults. MS thesis, Massachusetts Institute of Technology, Cambridge, MA.

Moriya, H., Fujita, T., Niitsuma, H., Eisenblätter, J., and Manthei, G. (2006). "Analysis of fracture propagation behavior using hydraulically induced acoustic emissions in the Bernburg salt mine, Germany." *Int. J. Rock Mech. Min. Sci*., 43(1), 49–57.

Mostyn, G. R., and Li, K. S. (1993). "Probabilistic slope analysis – State-of-play." *Proc. of the Conf. on Probabilistic Methods in Geotechnical Engineering*, Lanberra, Australia, 89-109.

Nicol, A., Watterson, J., Walsh, J. J., and Childs, C. (1996). "The shapes, major axis orientations and displacement patterns of fault surfaces." *Journal of Structural Geology*, 18(2/3), 235-248.

Petit, J.-P., Massonnat, G., Pueo, F., and Rawnsley, K. (1994). "Rapport de forme des fractures de mode 1 dans les roches stratifiees: Une etude de cas dans le Bassin Permian de Lodeve (France)." *Bulletin du Centre de Recherches Elf Exploration Production*, 18(1), 211-229.

Pollard, D.D., and Aydin, A.A. (1988). "Progress in Understanding Jointing over the Past Century." *Geological Society of America Bulletin*. 1001, 1181-1204.

Price, N. J. (1966). *Fault and Joint Development in Brittle and Semi Brittle Rock*. Pergamon Press, London, 176 pp.

Riedel, W. (1929). "Zur Mechanik Geologischer Brucherscheinungen." *Zentrabl, Mineral*, Abt. B., 354-68.

Rippon, J. H. (1985a). "Contoured patterns of the throw and hade of normal faults in the Coal Measures (Westphalian) of north-east Derbyshire." *Proc. Yorks. Geol. Soc*., 45, 147-161.

Rippon, J. H. (1985b). "New methods of forecasting the throw and hade of faults in some North Derbyshire Collieries." *Trans. Inst. Min. Engrs*., 145, 198-204.

Robertson, A. (1970). "The interpretation of geologic factors for use in slope theory." *Proc., Symp. on the Theoretical Background to the Planning of Open Pit Mines*, Johannesburg, South Africa, 55-71.

Saltzman, B. (2001). *Possible correlation between mechanical layer's joint spacing and its rock mechanical properties*. M.S. Thesis, Ben Gurion University of the Negev.

Savalli, L., and Engelder T. (2005). "Mechanisms controlling rupture shape during subcritical growth of joints in layered rocks." *GSA Bulletin*, 117(3/4), 436-449.

Sheldon, P. (1912). “Some Observations and Experiments on Joint Planes.” *J. Geol.*, 20, 164-183.

Song, J.-J. (2006). “Estimation of areal frequency and mean trace length of discontinuities observed in non-planar surfaces.” *Rock Mechanics and Rock Engineering*, 39(2), 131-146.

Song, J.-J., and Lee, C.-I. (2001). “Estimation of joint length distribution using window sampling.” *Int. J. Rock Mech. Min. Sci*., 38(4), 519–528.

Villaescusa, E., and Brown, E. T. (1990). “Maximum likelihood estimation of joint size from trace length measurements.” *Rock Mechanics and Rock Engineering*, 25, 67-87.

Warburton, P. M. (1980a). “A stereological interpretation of joint trace data.” *Int. J. Rock Mech. Min. Sci. & Geomech. Abstr*., 17, 181-190.

Warburton, P. M. (1980b). “Stereological interpretation of joint trace data: Influence of joint shape and implications for geological surveys.” *Int. J. Rock Mech. Min. Sci. & Geomech. Abstr*., 17, 305-316.

Walsh, J. J., and Watterson, J. (1989). “Displacement gradients on fault surfaces.” *J. Struct. Geol*., 11, 307-316.

Wathugala, D. N. (1991). "Stochastic three dimensional joint geometry modeling and verification." PhD Dissertation, University of Arizona, Tucson, Arizona.

Weinberger, R. (2001). "Joint nucleation in layered rocks with non-uniform distribution of cavities." *J. Struct. Geol*., 23, 1241-1254.

Woodworth, J. B. (1896). "On the Fracture System of Joints, with Remarks on Certain Great Fractures." *Boston Society of Natural History, Proc.*, 27, 163-184.

Zhang, L. (1999). *Analysis and Design of Drilled Shafts in Rock*. PhD Dissertation, Massachusetts Institute of Technology, Cambridge, MA.

Zhang, L. (2005). *Engineering Properties of Rocks*. Elsevier, p304.

Zhang, L., Einstein, H. H., and Dershowitz, W. S. (2002). "Stereological relationship between trace length distribution and size distribution of elliptical discontinuities." *Geotechnique*, London, UK, 52(6), 419-433.

Table 1. Mean of strike trace lengths and mean of dip trace lengths of two discontinuity sets (from Einstein et al. 1979)

Discontinuity Set #	Mean of strike trace lengths (ft.)	Mean of dip trace lengths (ft.)
1	28.3	16.1
2	25.2	21.1

Table 2. Details of the four data sets plotted in Fig. 8 (from Nicol et al. 1996)

Name and location	Lithologies	Number of faults	Aspect ratio (average)
Derbyshire Coal Mines, UK	Carboniferous sandstone, shale and coal	12	2.3
Timor Sea	Cenozoic limestone, claystone and sandstone	9	2.2
Gulf Coast	Late Miocene to recent sandstone with minor shales	7	1.6
North Sea	Jurassic sandstone and shales	7	2.4

Notes: 1) Aspect ratio is the major to minor axis ratio of the approximately elliptical faults.

2) Data from the Derbyshire Coal field are from coal-seam planes, the remainder are from two- and three-dimensional offshore reflection seismic data sets.

Table 3. Expressions for determining the mean μ_l and standard deviation σ_l of trace lengths from the mean μ_a and standard deviation σ_a of discontinuity size a

Distribution form of $g(a)$	μ_l	$(\sigma_l)^2$
Lognormal	$\frac{\pi M[(\mu_a)^2+(\sigma_a)^2]}{4\mu_a}$	$\frac{32M^2[(\mu_a)^2+(\sigma_a)^2]^3 - 3\pi^2M^2(\mu_a)^2[(\mu_a)^2+(\sigma_a)^2]^2}{48(\mu_a)^4}$
Negative exponential	$\frac{\pi M}{2}\mu_a$	$\frac{(16-\pi^2)M^2}{4}(\mu_a)^2$
Gamma	$\frac{\pi M[(\mu_a)^2+(\sigma_a)^2]}{4\mu_a}$	$\frac{32M^2[(\mu_a)^2+(\sigma_a)^2][(\mu_a)^2+2(\sigma_a)^2] - 3\pi^2M^2[(\mu_a)^2+(\sigma_a)^2]^2}{48(\mu_a)^2}$

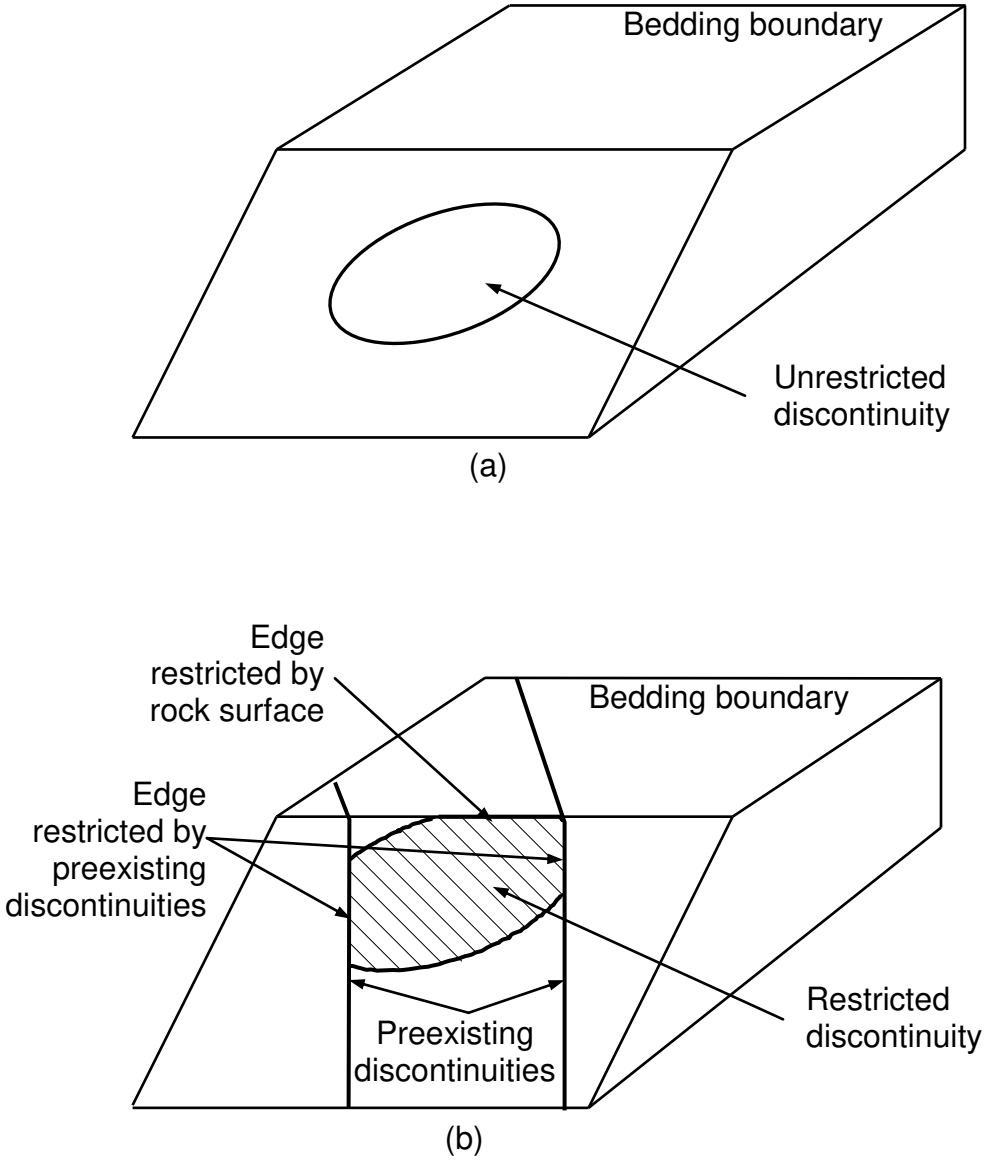

Fig.1. (a) An unrestricted discontinuity; (b) A restricted discontinuity;

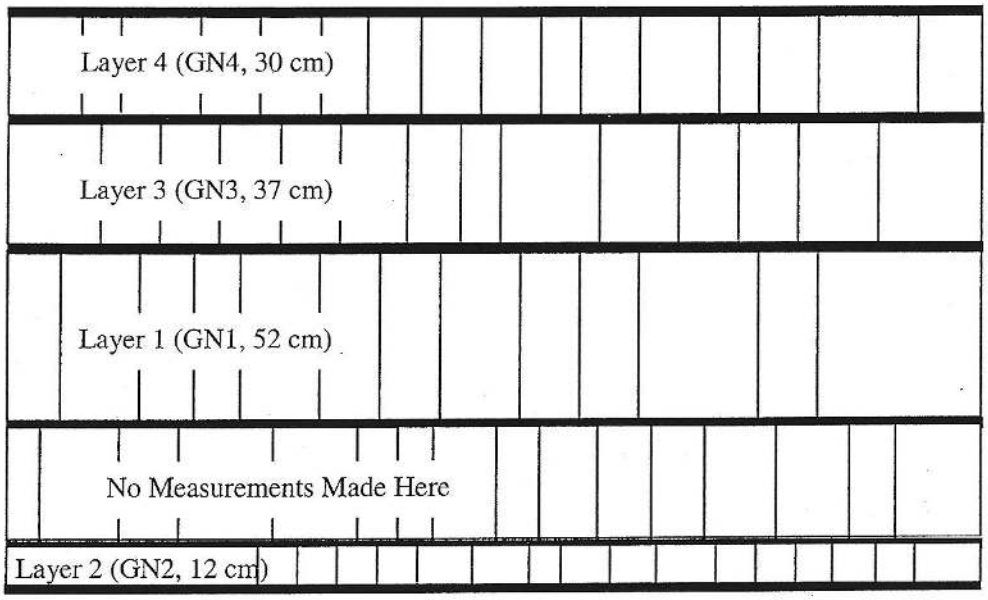

Fig.1. (c) Layer Perpendicular Joints. A Particular Case of Restricted Joints. Schematic of the Limestone/Dolostone Layers Studied by Saltzman (2001) (Sketched by Locsin 2005 from a Photograph in Saltzman, 2001). The Layers are Bounded by Marlsone (represented by Dark Solid Lines).

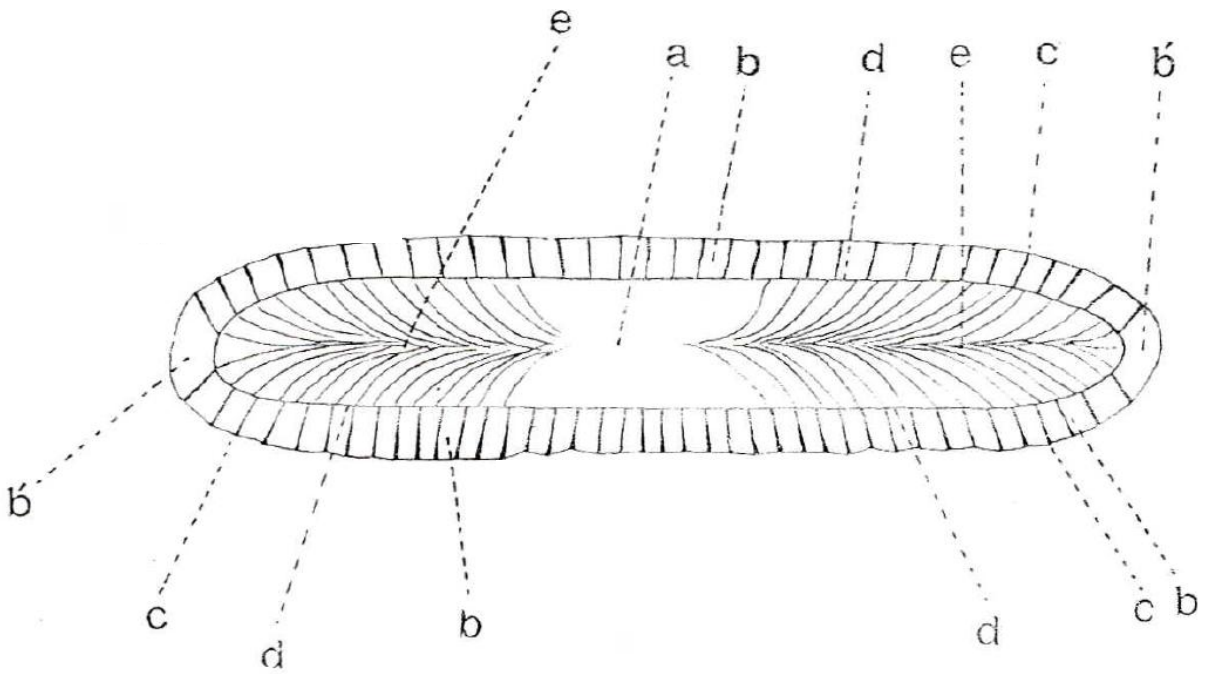

(A)

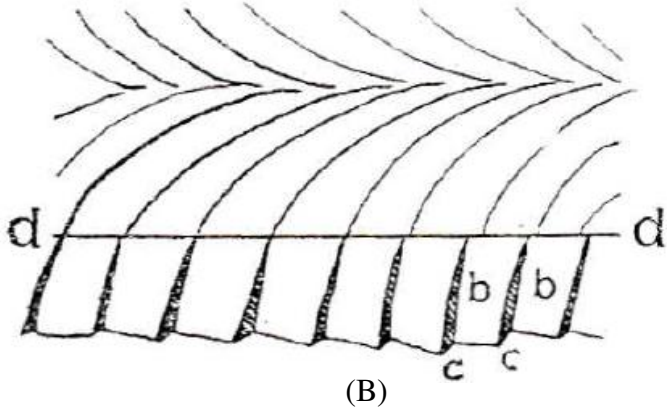

(B)

Fig. 2. Drawings of surface markings and profiles of joints in Cambridge Argillite: (A) The entire joint surface (a = center, b = border, c = cross fractures, d = edge of joint plane = inner margin of fringe, e = axis of feather fractures); (B) Joint fringe region (b) with echelon joint segments (c) (from Woodworth 1896 Plate 1, Fig. 10 (A in this figure), Fig. 5. (B in this Figure)).

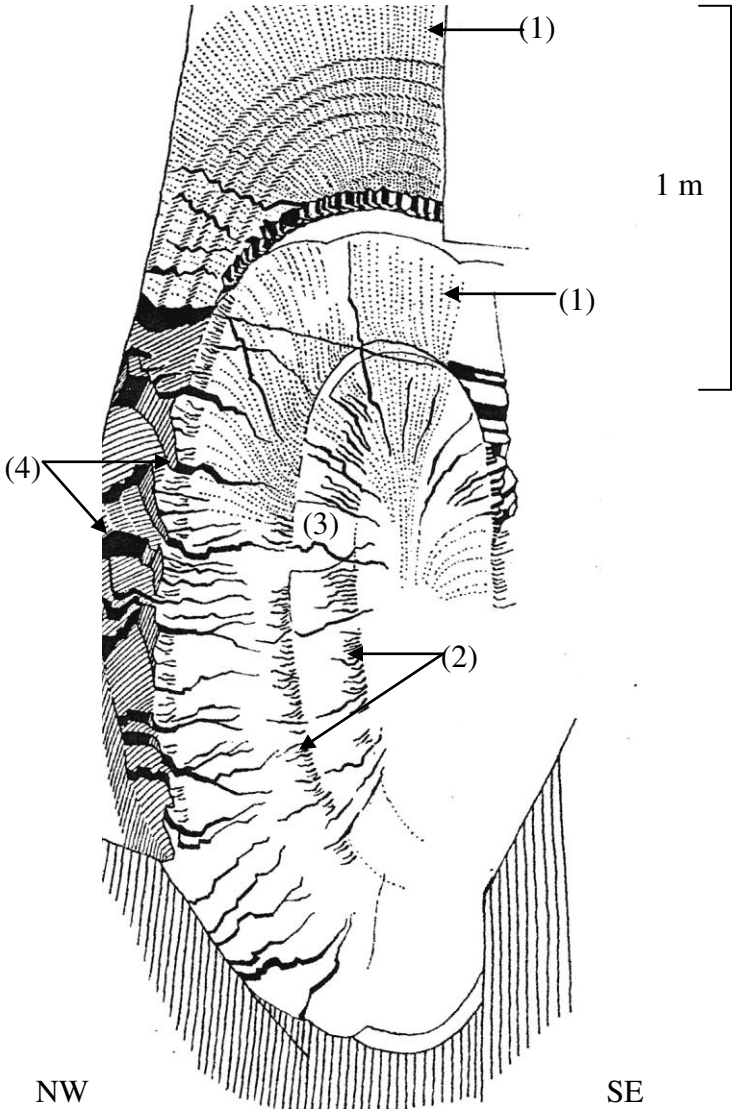

Fig. 3. Joint with plumose (1) and ring structures (2), radial (3) and boundary joints (4), which lead over to en-echelon jointing. The plumose structures are only indicated in the upper part. Griffelschiefer (schist) from the schist quarries at the Trebenkopf, west of Oberwirbach (Sheet Bad Blankenburg). This figure is Fig. 5 in Bankwitz (1965). The legend has been translated from the German original. The numbers in parentheses and the numbers in the figure which identify the various features have been added by the authors of this paper.

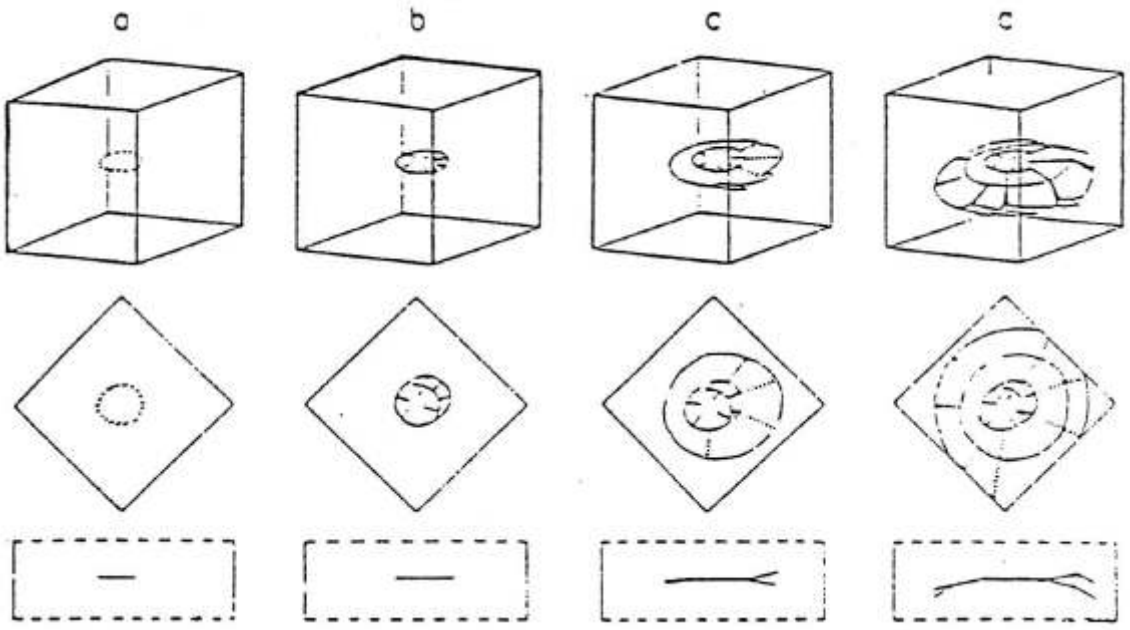

Fig. 4. Development of **a joint** according to Bankwitz (1966).

Figures a-d represent different times in the joint development (mm to m size); from top to bottom – 3-d view; top view; side view. The "rings" correspond to those in Fig. 3 and delimit zones of simultaneous propagation.

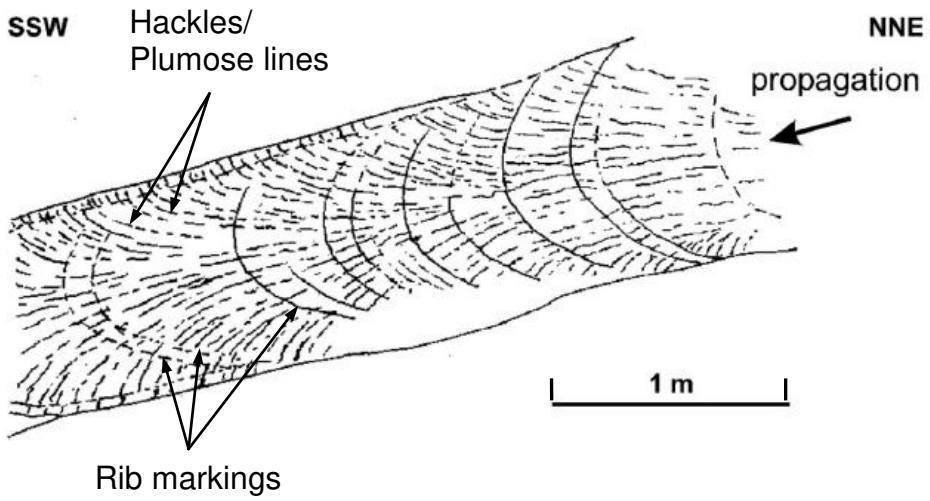

Fig. 5. Elliptical propagation of fracture confined by two subhorizontal boundaries (above and below) (from Bahat 2003).

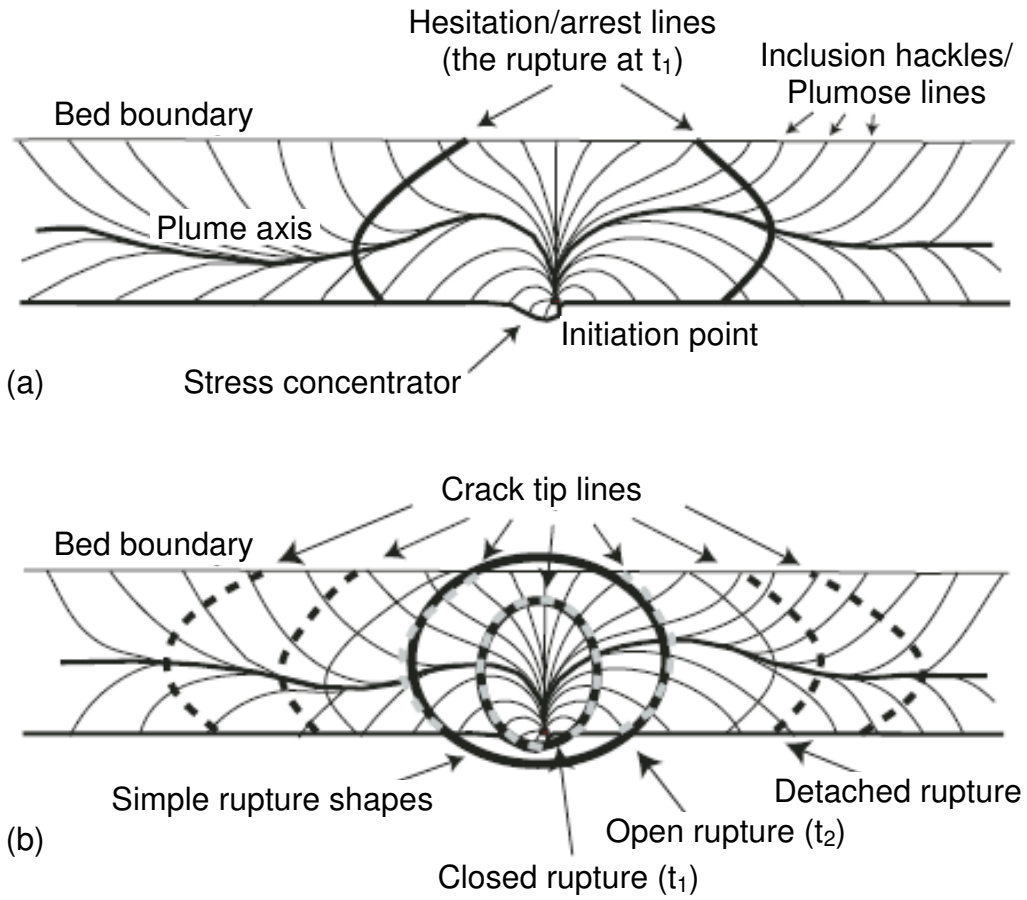

Fig. 6. (a) Natural features on joint surfaces. Joints initiate at and propagate away from a stress concentration point. Plumes (i.e. barbs, inclusion hackles, striae, plume lines) diverge from the initiation point in the propagation direction. Arrest lines form at right angles to plumes where the crack tip hesitated or arrested. (b) Interpretive features on joint surfaces. Crack tip lines are the dashed curves drawn perpendicularly to plume traces. Rupture shapes coincide with the trace of the crack tip line at three stages of rupture growth, t_i (i = 1, 2, 3) (from Savalli and Engelder 2005).

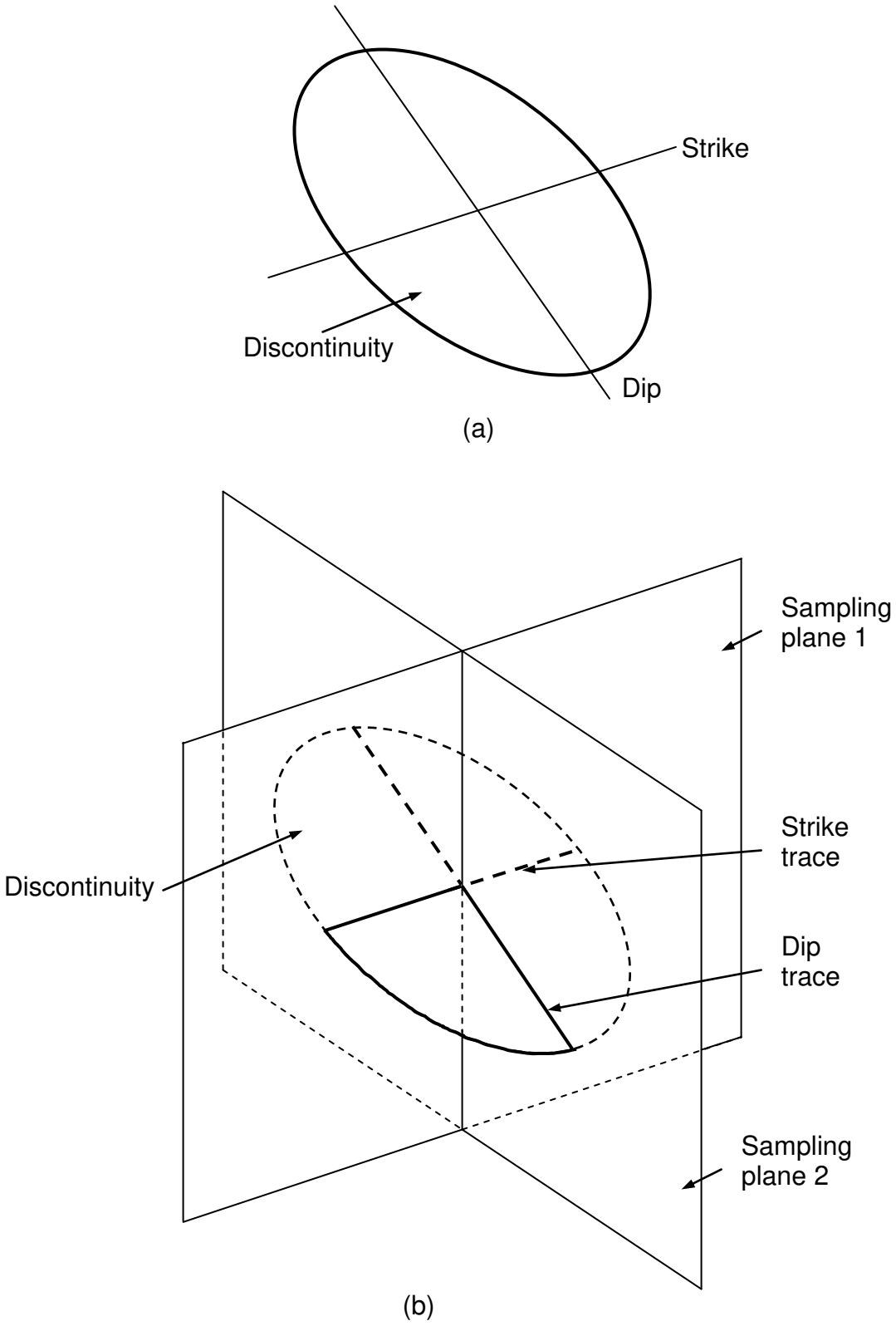

Fig. 7. (a) Strike and dip of a discontinuity; and (b) Strike and dip traces

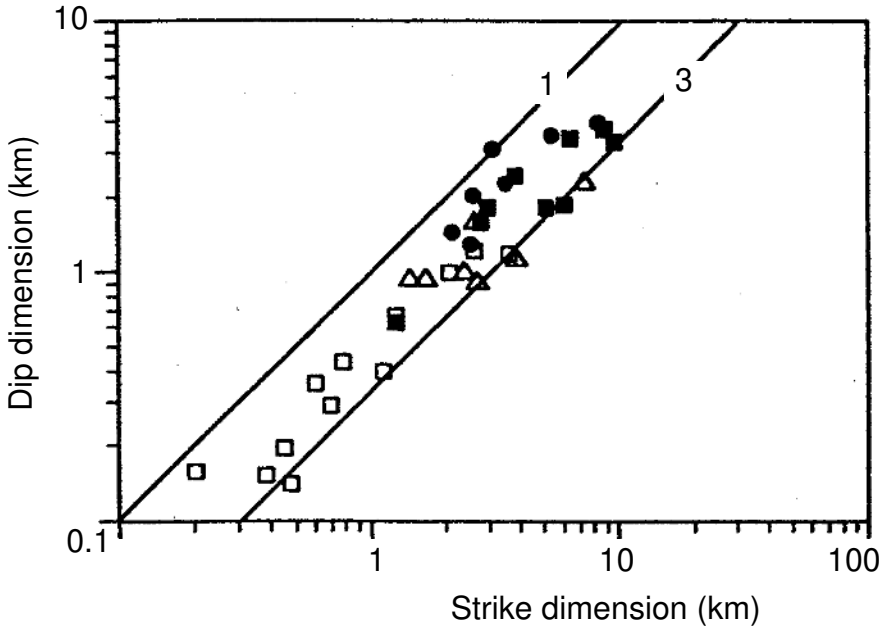

Fig. 8. Dip dimension versus strike dimension of **normal** faults from four regions (see Table 2) (from Nicol et al. 1996)

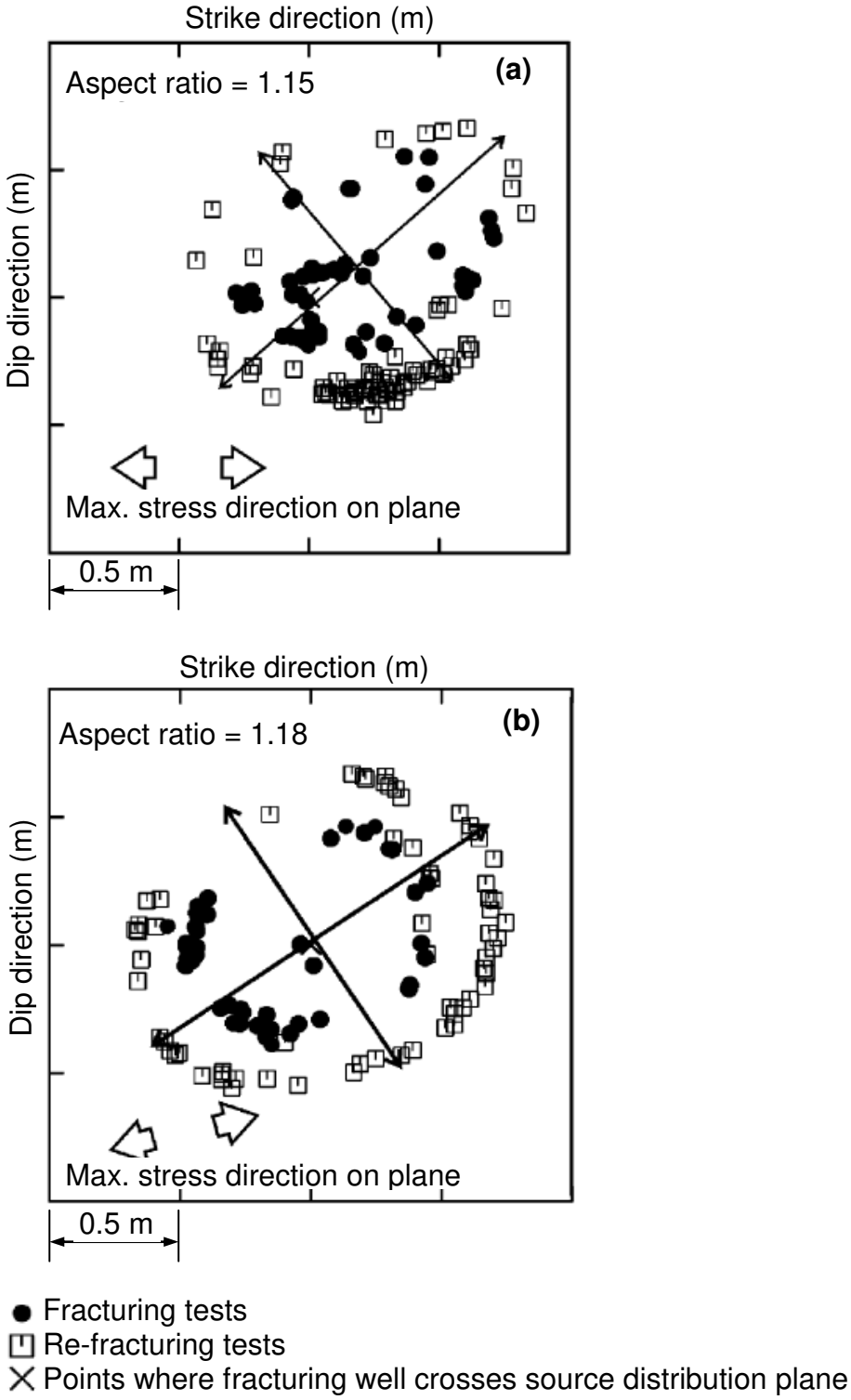

Fig. 9. Acoustic emission (AE) source locations at (a) fracturing point FS2; and (b) fracturing point FS5 (from Moriya et al. 2006)

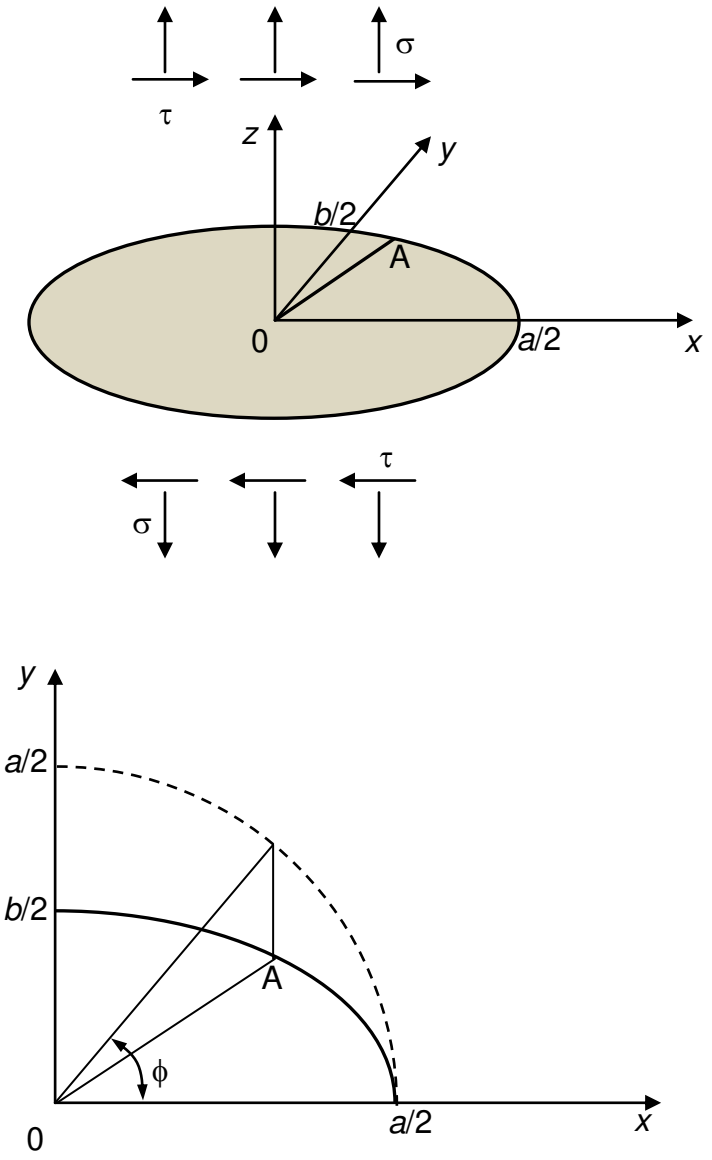

Fig. 10. A two-dimensional elliptical fracture with normal and shear stress acting on it (after Moriya et al. 2006)

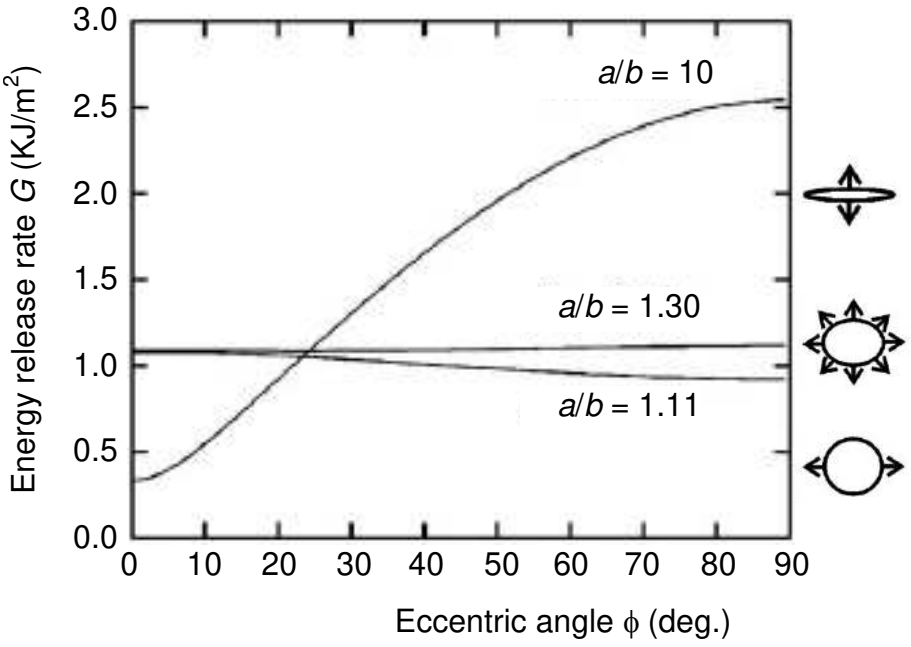

Fig. 11. Variation of energy release rate with eccentric angle at aspect ratio values of 10, 1.30 and 1.11 (after Moriya et al. 2006)

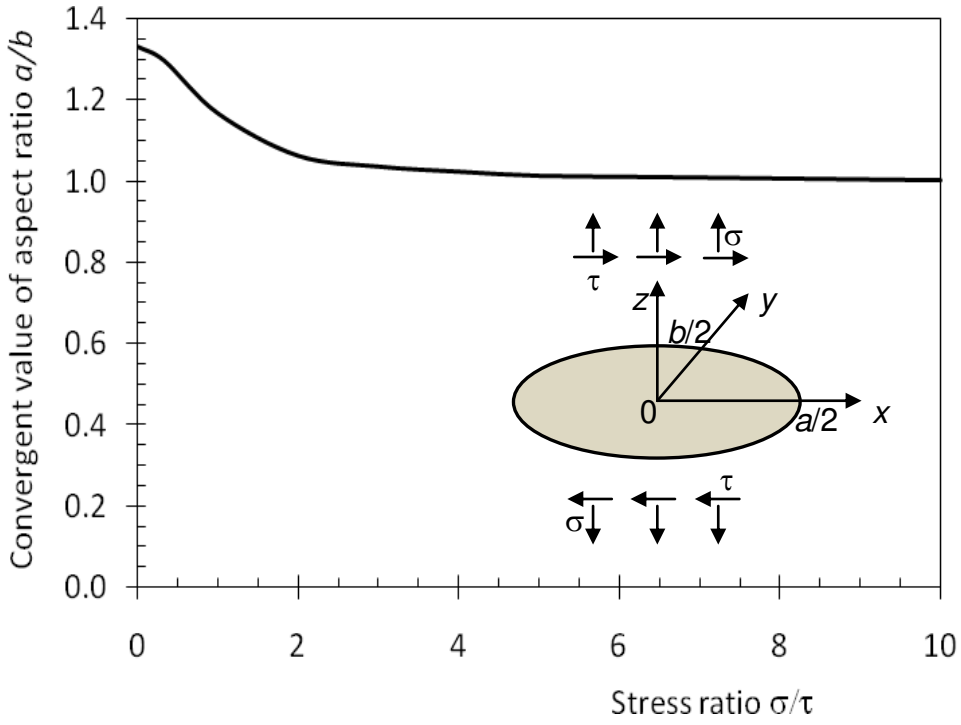

Fig. 12. Relationship between stress ratio and convergent value of aspect ratio (after Moriya et al. 2006)

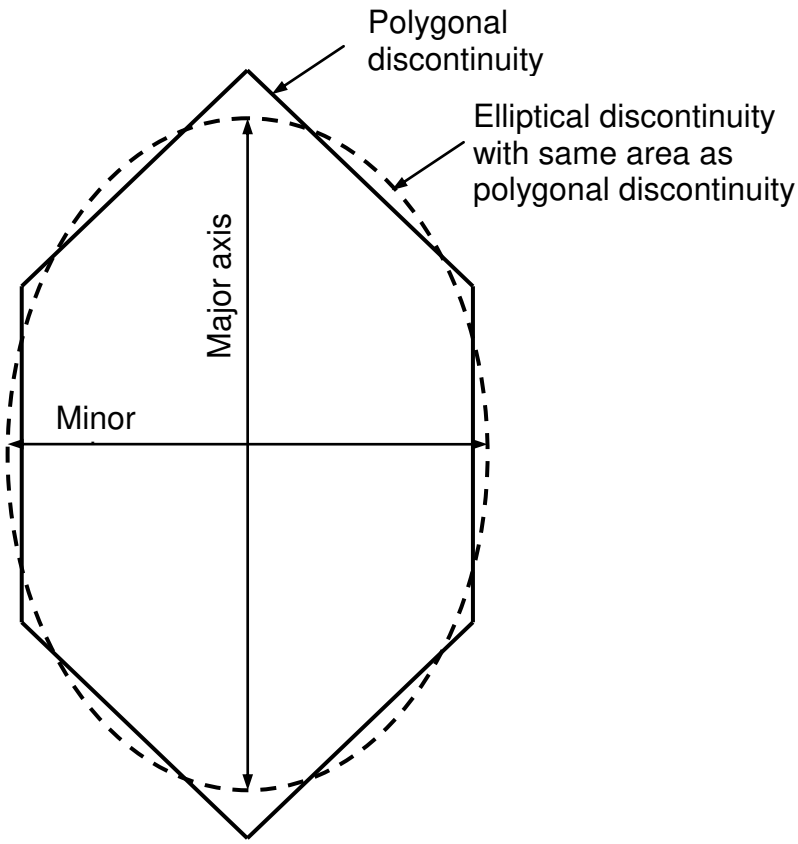

Fig. 13. A polygon is used to represent an elliptical discontinuity (fracture) (from Dershowitz et al. 1993)

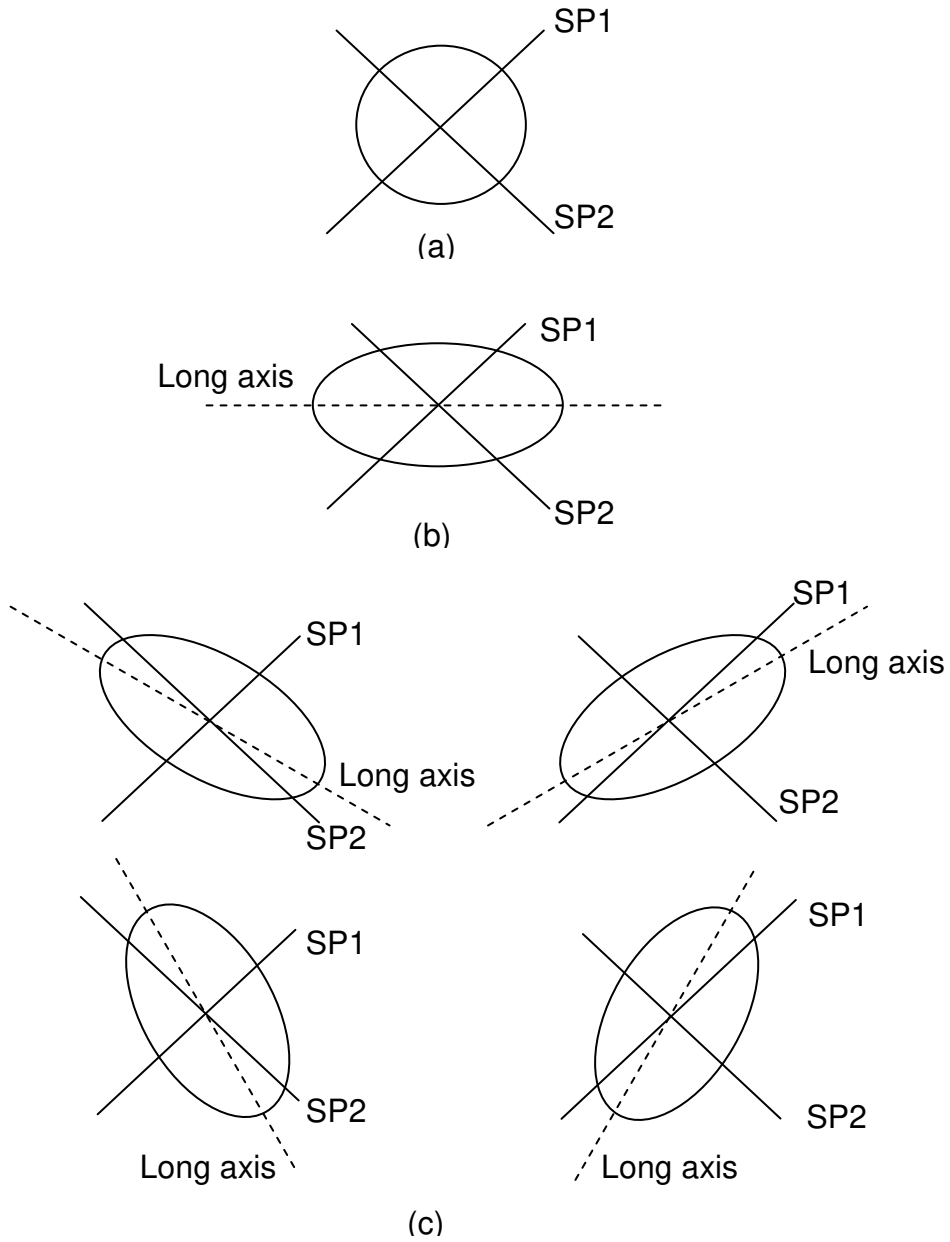

Fig. 14. Three possible cases for which the average trace lengths on two sampling planes are about equal: (a) Discontinuities are equidimensional (circular); (b) Discontinuities are non-equidimensional (elliptical), with long axes in a single orientation. The two sampling planes, SP1 and SP2, are oriented in such a way that the trace lengths on them are about equal; and (c) Discontinuities are non-equidimensional (elliptical), with long axes randomly orientated. The two sampling planes, SP1 and SP2, are oriented in such a way that the average trace lengths on them are about equal.

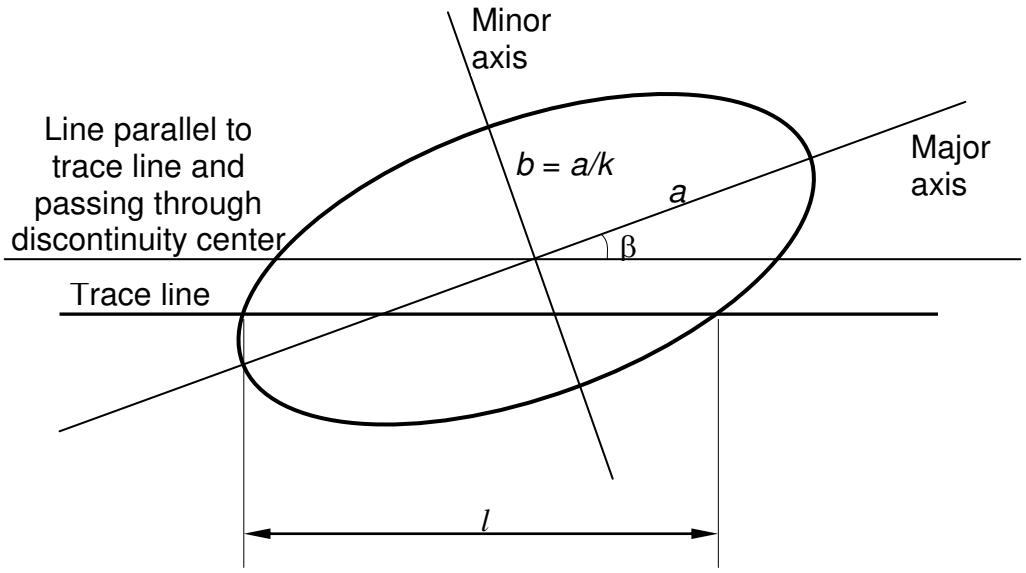

Fig. 15. Parameters used in the definition of an elliptical discontinuity (after Zhang et al. 2002)

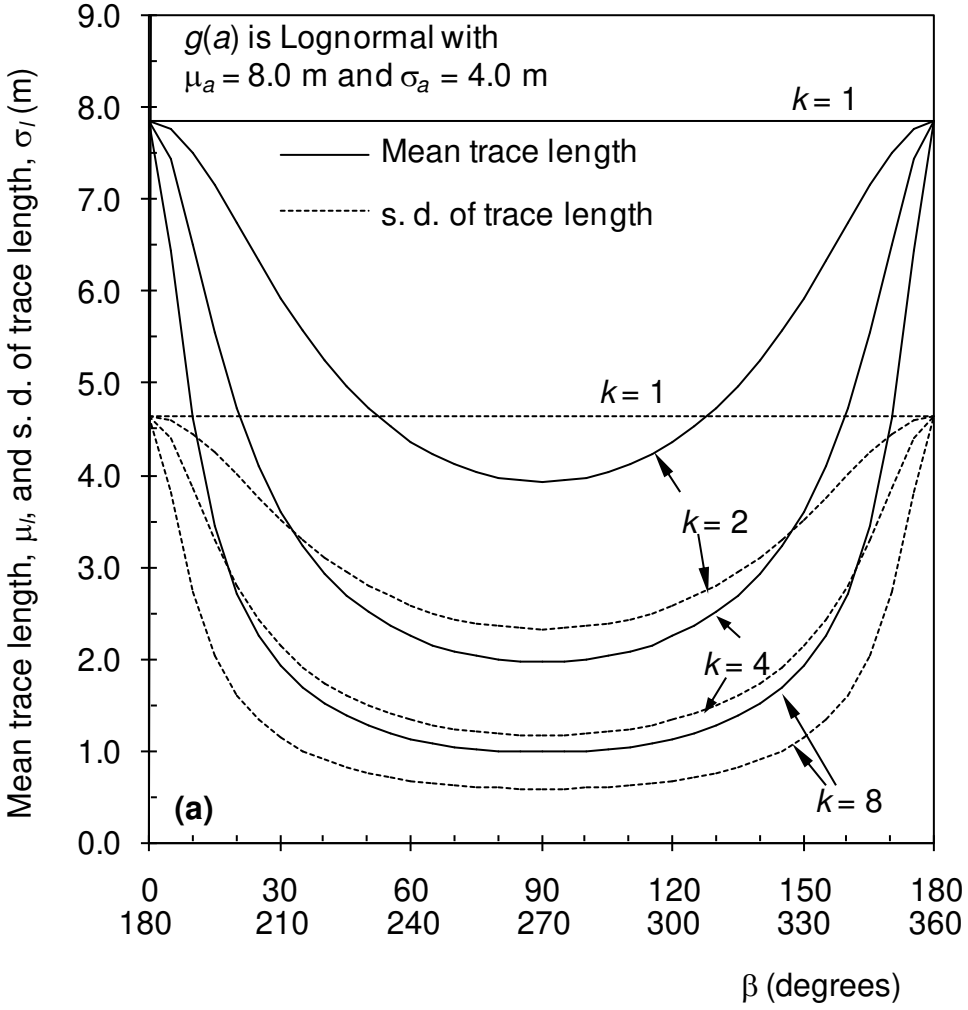

Fig. 16. Variation of mean and standard deviation (s.d.) of trace length with β for different distributions of discontinuity size *a*: (a) Lognormal; (b) Negative exponential; and (c) Gamma.

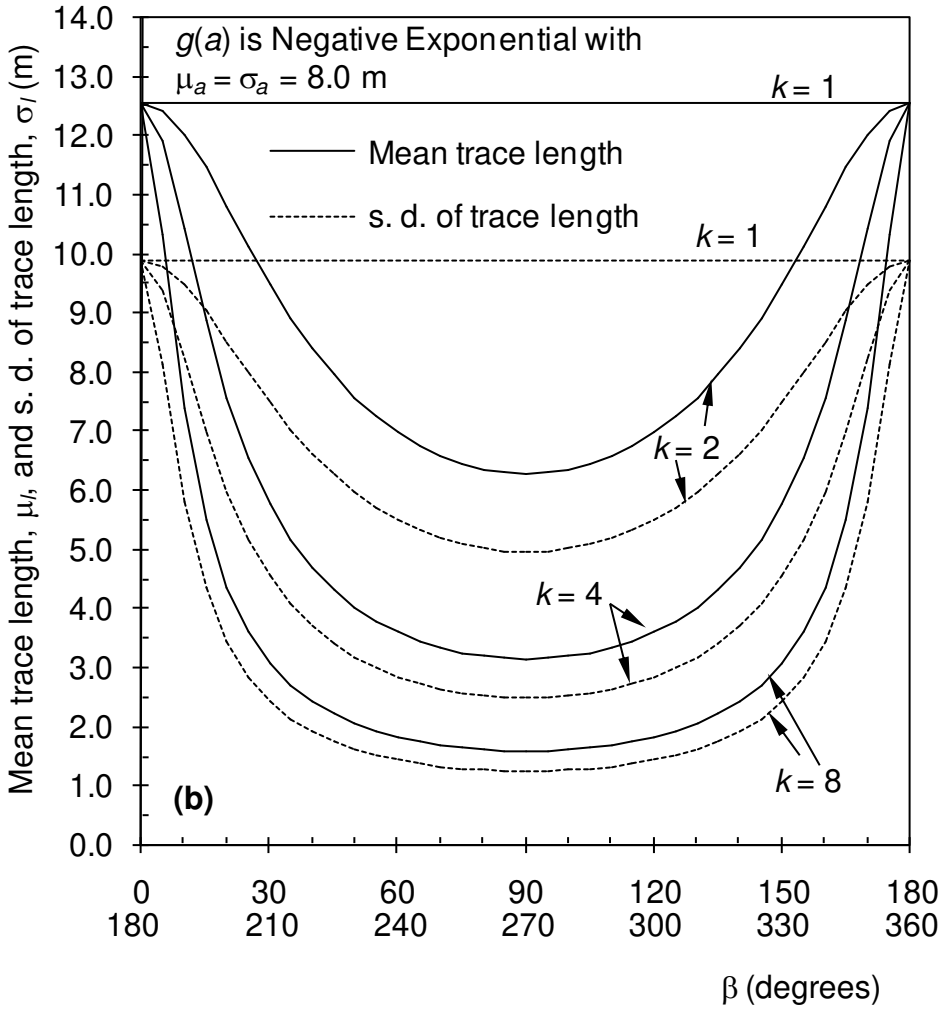

Fig. 16. Variation of mean and standard deviation (s.d.) of trace length with β for different distributions of discontinuity size *a*: (a) Lognormal; (b) Negative exponential; and (c) Gamma.

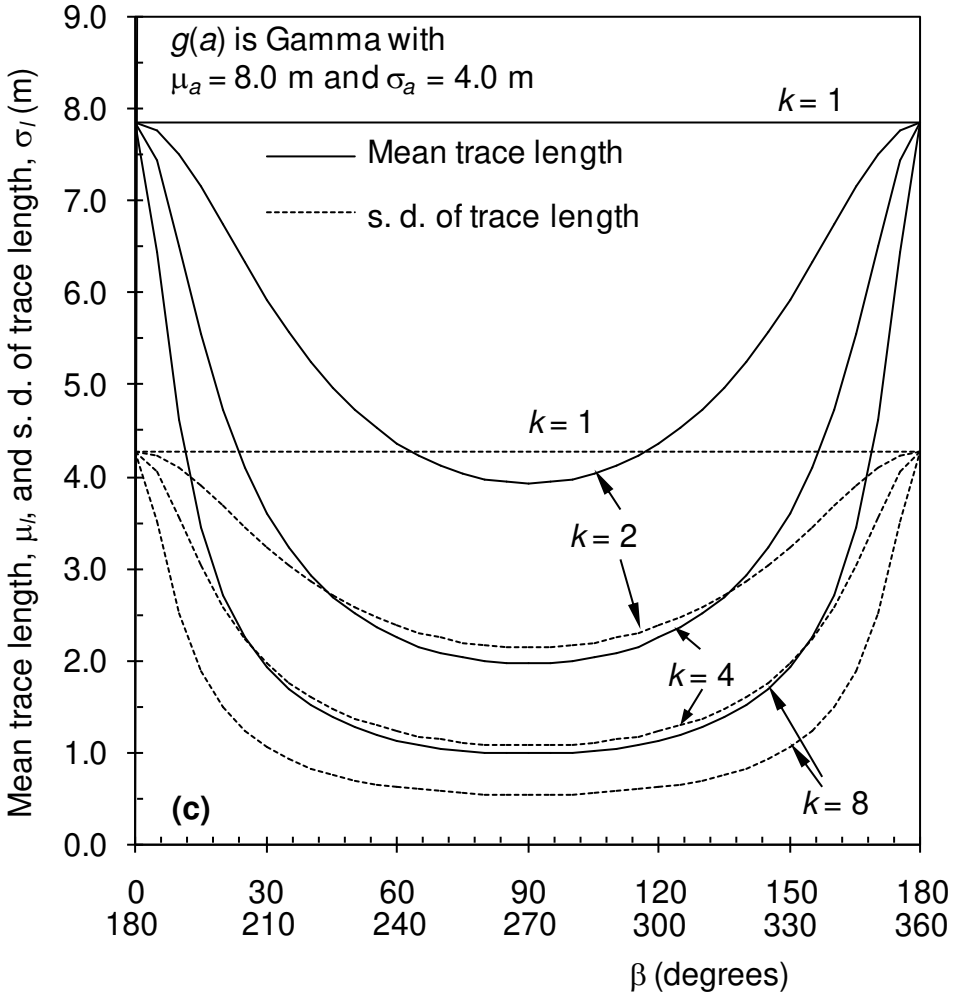

Fig. 16. Variation of mean and standard deviation (s.d.) of trace length with β for different distributions of discontinuity size *a*: (a) Lognormal; (b) Negative exponential; and (c) Gamma.

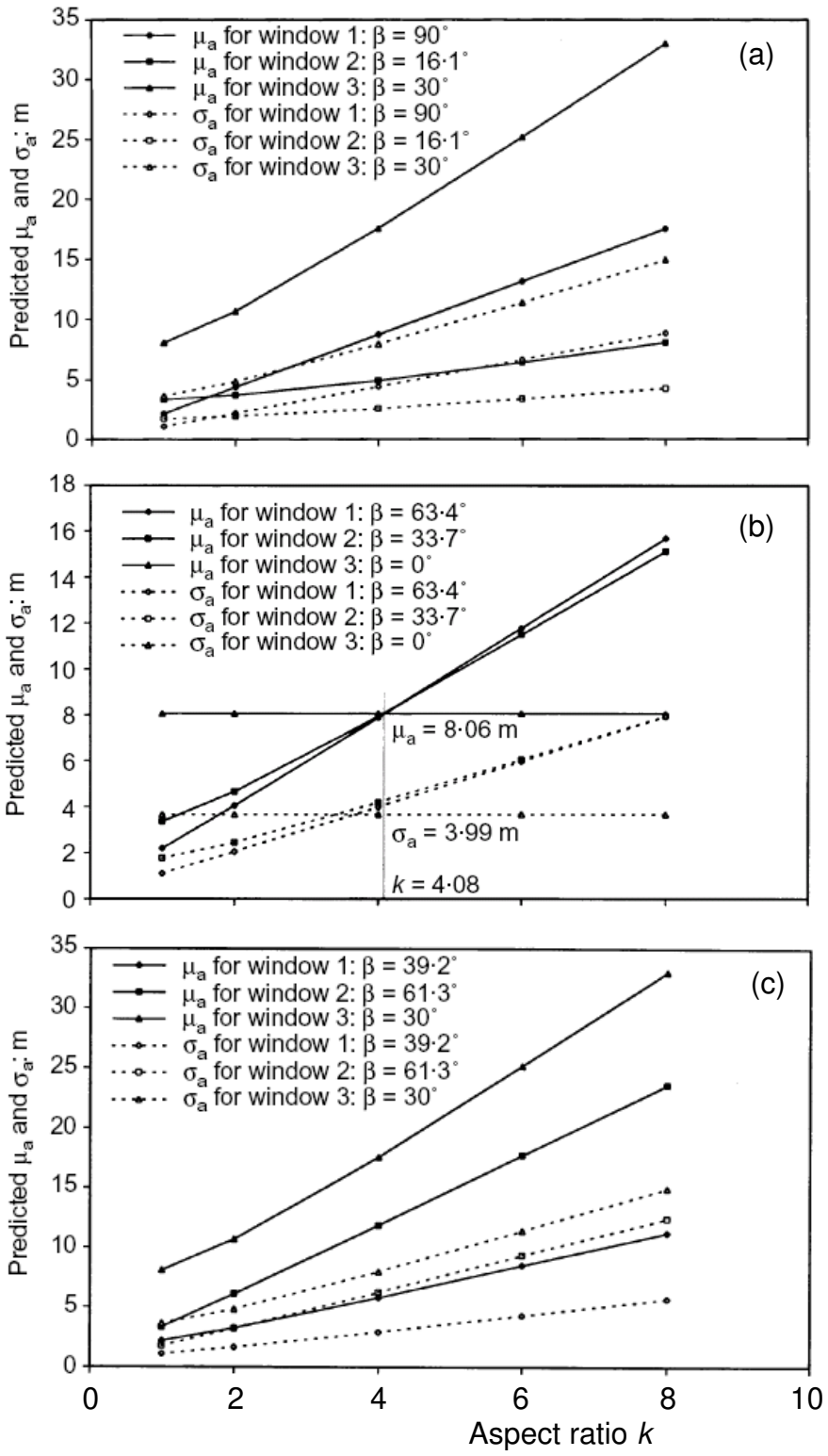
(a)
μ_a for window 1: β = 90°
μ_a for window 2: β = 16·1°
μ_a for window 3: β = 30°
σ_a for window 1: β = 90°
σ_a for window 2: β = 16·1°
σ_a for window 3: β = 30°
Predicted μ_a and σ_a: m
(b)
μ_a for window 1: β = 63·4°
μ_a for window 2: β = 33·7°
μ_a for window 3: β = 0°
σ_a for window 1: β = 63·4°
σ_a for window 2: β = 33·7°
σ_a for window 3: β = 0°
μ_a = 8·06 m
σ_a = 3·99 m
k = 4·08
(c)
μ_a for window 1: β = 39·2°
μ_a for window 2: β = 61·3°
μ_a for window 3: β = 30°
σ_a for window 1: β = 39·2°
σ_a for window 2: β = 61·3°
σ_a for window 3: β = 30°
Aspect ratio k

Fig. 17. Variation of μ_a and σ_a with aspect ratio k for assumed major axis orientation of (a) 0°/0°; (b) 30°/0°; and (c) 60°/0° (after Zhang et al. 2002)**; assuming a lognormal distribution of g(a)**.

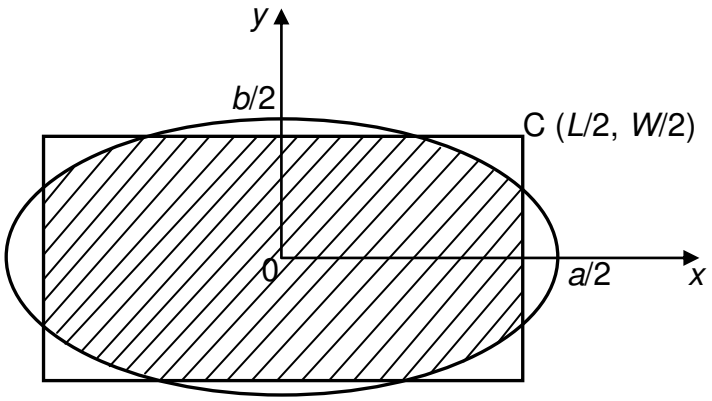

Ellipse and rectangle have the same area and the same aspect ratio, i.e. $\pi ab = LW$ and $a/b = L/W = k$, which lead to $L = (\sqrt{\pi}/2)a$ and $W = (\sqrt{\pi}/2)b$

Fig. 18. Representing a rectangle by an ellipse with the same area and the same aspect ratio.